AD-A044 791 BALLISTIC RESEARCH LABS ABERDEEN PROVING GROUND MD F/G 20/2
SHOCK PROPAGATION IN THE ONE-DIMENSIONAL LATTICE,(U)
AUG 77 J D POWELL, J H BATTEH
UNCLASSIFIED BRL-2009 NL

| OF |
ADA044791

END
DATE FILMED
10-77
DDC

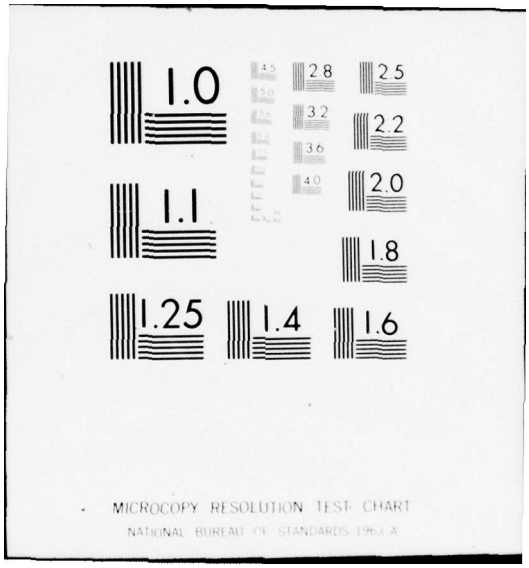
1.0
1.1
1.25
1.4
1.6
1.8
2.0
2.2
2.5
2.8
3.2
3.6
4.0
4.5
5.0
MICROCOPY RESOLUTION TEST CHART
NATIONAL BUREAU OF STANDARDS 1963-A

BRL

(12) NW

AD

REPORT NO. 2009

SHOCK PROPAGATION IN THE ONE-DIMENSIONAL LATTICE

John D. Powell
Jad H. Batteh

August 1977

USA ARMAMENT RESEARCH AND DEVELOPMENT COMMAND
USA BALLISTIC RESEARCH LABORATORY
ABERDEEN PROVING GROUND, MARYLAND

Destroy this report when it is no longer needed.
Do not return it to the originator.

Secondary distribution of this report by originating or sponsoring activity is prohibited.

Additional copies of this report may be obtained from the National Technical Information Service, U.S. Department of Commerce, Springfield, Virginia 22151.

The findings in this report are not to be construed as an official Department of the Army position, unless so designated by other authorized documents.

The use of trade names or manufacturers' names in this report does not constitute indorsement of any commercial product.

UNCLASSIFIED

SECURITY CLASSIFICATION OF THIS PAGE *(When Data Entered)*

REPORT DOCUMENTATION PAGE		READ INSTRUCTIONS BEFORE COMPLETING FORM
1. REPORT NUMBER BRL Report No. 2009	2. GOVT ACCESSION NO.	3. RECIPIENT'S CATALOG NUMBER
4. TITLE *(and Subtitle)* Shock Propagation in the One-Dimensional Lattice		5. TYPE OF REPORT & PERIOD COVERED
		6. PERFORMING ORG. REPORT NUMBER
7. AUTHOR(s) John D. Powell and Jad H. Batteh		8. CONTRACT OR GRANT NUMBER(s)
9. PERFORMING ORGANIZATION NAME AND ADDRESS Ballistic Research Laboratory Aberdeen Proving Ground, MD 21005		10. PROGRAM ELEMENT, PROJECT, TASK AREA & WORK UNIT NUMBERS 1L161102AH43
11. CONTROLLING OFFICE NAME AND ADDRESS US Army Materiel Development & Readiness Command 5001 Eisenhower Avenue Alexandria, VA 22333		12. REPORT DATE AUGUST 1977 13. NUMBER OF PAGES 84
14. MONITORING AGENCY NAME & ADDRESS*(if different from Controlling Office)*		15. SECURITY CLASS. *(of this report)* Unclassified 15a. DECLASSIFICATION/DOWNGRADING SCHEDULE

16. DISTRIBUTION STATEMENT *(of this Report)*

Approved for public release; distribution unlimited.

17. DISTRIBUTION STATEMENT *(of the abstract entered in Block 20, if different from Report)*

18. SUPPLEMENTARY NOTES

19. KEY WORDS *(Continue on reverse side if necessary and identify by block number)*

Shock Propagation, Lattice Dynamics, Computer Molecular Dynamics, Solitons, Nonequilibrium phenomena

20. ABSTRACT *(Continue on reverse side if necessary and identify by block number)* (hmn)

Shock propagation in a one-dimensional, discrete lattice is studied in some detail both by reviewing existing treatments of the problem and by providing a number of extensions to those treatments. Although some analytic work is presented, most of the study is in the form of a computer simulation. The purpose of the simulation is to solve numerically the classical equations of motion of the atoms of the lattice as they respond to the shock wave. Various forms of interatomic potential are considered and the resulting differences are noted and

DD FORM 1 JAN 73 1473 EDITION OF 1 NOV 65 IS OBSOLETE

UNCLASSIFIED

SECURITY CLASSIFICATION OF THIS PAGE (When Data Entered)

discussed. The effect of the initial state of the lattice upon the shock profile is studied by considering two sets of initial conditions. In the first, the atoms are at rest in their equilibrium positions prior to compression by the shock wave; in the second, the lattice is initially in thermal equilibrium at approximately room temperature. All anharmonic potentials studied are found to support the propagation of well-defined, stable pulses (solitons) and the physical implications of these rather unusual pulses are examined. Specific future investigations are recommended and their relevance to Army-related problems is explained.

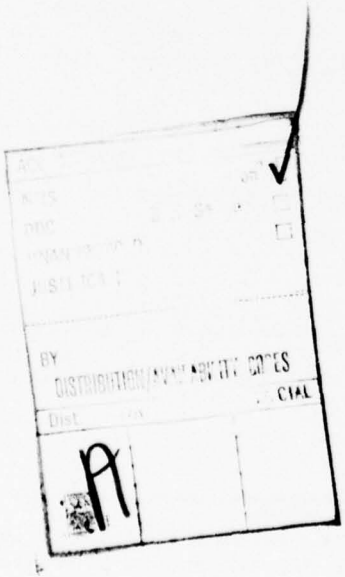

TABLE OF CONTENTS

LIST OF FIGURES

Figure Page

LIST OF TABLES

1. INTRODUCTION

The purpose of this report is to review, unify, and extend recent studies of shock propagation in monatomic, discrete crystal lattices. Most of these studies, undertaken by various investigators during the past decade or so, have employed computer-molecular-dynamic techniques to simulate the motion of the shock wave through the lattice, and this procedure will be largely followed in the present work. Although these "brute-force" techniques suffer from well-known limitations, the current state of the art is such that they provide the only practical way of treating highly nonlinear problems in lattice dynamics. The calculations of the report will be confined to a one-dimensional lattice. This limitation has been introduced partly because the one-dimensional lattice is considerably easier to treat numerically, partly because we believe that most of the physical principles are contained in such a model, and partly because it is desirable to investigate such questions as numerical accuracy before proceeding to more complicated, three-dimensional calculations.

The motivation for studying shock propagation from a microscopic point of view has been the belief that a continuum approach may fail, in certain cases, to predict the effect adequately. Early investigations of shock propagation in gases, using a hydrodynamic approach, revealed that for strong shock waves the shock thickness was of the order of a gas molecular mean free path[1]. This condition invalidates the use of the Navier-Stokes equations[2] and prompted investigators, most notably Mott-Smith[2], to reconsider the shock problem from the point of view of kinetic theory. More recently, investigations have been undertaken using computer-simulation methods[3].

An analagous approach for the case of shock waves in solids has proceeded much more slowly, owing primarily to the increased difficulty. For several reasons, however, the need for such an examination clearly exists.

---

1. R. Becker, "Stosswelle und Detonation", Z. Physik 8, 321 (1922).
2. H.M. Mott-Smith, "The Solution of the Boltzmann Equation for a Shock Wave", Phys. Rev. 82, 885 (1951).
3. G.A. Bird, "Aspects of the Structure of Strong Shock Waves", Phys. Fluids 13, 1172 (1970).

First, it is known that discrete lattices exhibit dispersion which is not accounted for in the hydrodynamic approach. For example, if a one-dimensional, harmonic lattice (linear interatomic forces) is subjected to steady compression, the resulting "shock" profile does not approach a steady state*. The reason is that the different normal-mode frequencies present in the compression wave travel at different group speeds; the higher-frequency modes travel more slowly than the lower-frequency modes and thus trail ever farther behind the head of the front. The effect is similar to the dispersive spreading of a quantum-mechanical wave packet. For more realistic anharmonic lattices (nonlinear interatomic forces), dispersion is complicated by the coupling between the various normal modes and it is important to determine the consequences of this coupling.

Second, a fluid-dynamical treatment of a solid can be valid only if material rigidity can be neglected. This condition is probably satisfied provided the pressure in the solid is much greater than the shear yield strength. While it is true that pressures behind strong shock fronts are much greater than the static yield strength, it would be more appropriate to compare them with the yield strength under dynamic conditions. As Tsai[4] has pointed out, the yield strength then is probably much greater than in the static case, perhaps approaching the theoretical strength.

Third, continuum treatments of shock propagation are dependent upon assumptions about equations of state for the solid under consideration as well as assumptions about the nature of viscous effects[5,6]. The equations of state are inadequately known for solids and the origin of viscous effects not completely understood. By use of computer simulations, one evades the necessity for these *a priori* assumptions.

---

*A harmonic lattice cannot support a shock wave in the usual sense for reasons discussed in the following section. We shall nevertheless use this terminology to refer to the resulting compression profile when the lattice is subjected to compression.

4. D.H. Tsai, "An Atomistic Theory of Shock Compression of a Perfect Crystalline Solid", in Accurate Characterization of the High-Pressure Environment, edited by E.C. Lloyd, Natl. Bur. Stds. Spec. Publ. No. 326 (U.S. GPO, Washington, DC, 1971), p. 105.
5. W. Band, "Studies in the Theory of Shock Propagation in Solids", J. Geophys. Res. 65, 695 (1960).
6. D.R. Bland, "On Shock Structure in a Solid", J. Inst. Math. Applications 1, 56 (1965).

Finally, since the classic computer study undertaken by Fermi, Pasta, and Ulam[7], considerable speculation has arisen about the manner in which crystal lattices approach thermal equilibrium. The hydrodynamic theory assumes that thermal equilibrium exists behind the shock and allows for only small deviations from equilibrium within the front. It is clearly important to examine the validity of these assumptions and they will be addressed in some detail in this report.

An attempt to resolve the points in the above discussion appears to be of special importance with regard to Army-related problems. For example, the Zeldovich-von Neumann-Doring (ZND) theory of detonation[8], probably the most widely used theory of shock-induced detonation, is based on the assumption that the details of the shock front can be ignored. In the ZND theory, the only effect of the shock is to raise the temperature, density, and pressure of the lattice to values higher than in the undisturbed lattice. Chemical reactions are then assumed to occur in the thermally equilibrated region behind the shock front. However, if the shock profile is not steady, or if the approach to equilibrium is not much more rapid than the times required for chemical reaction, the above assumption must clearly be called into question.

Before turning to the present calculations, we will briefly summarize the existing work as well as indicate some of the questions that it has raised. The most extensive studies of shock propagation in discrete lattices have been undertaken by Tsai and coworkers[4,9,10] over the last decade. Their more recent computer codes solve the atomic equations of motion for three-dimensional, face- and body-centered cubic crystals subjected to shock compression. An essential conclusion of their work is that the shock profile is not steady in time, but that the leading edge of the thermally equilibrated region behind the shock propagates more slowly than does the front itself. Consequently, the transition region grows wider in time. The nonsteady behavior has been interpreted by these investigators as being a natural extension of the low-temperature phenomenon of second sound[11,12]. However, a number of questions arise regarding this inter-

7. E. Fermi, J.R. Pasta, and S.M. Ulam, "Studies in Nonlinear Problems", Los Alamos Sci. Lab. Rep. LA-1940, 1955; also in Collected Works of Enrico Fermi (Univ. Chicago Press, Chicago, 1965), V. II, p. 978.
8. B. Lewis and G. von Elbe, Combustion, Flames, and Explosion of Gases (Academic, New York, 1951), Chap. XI.
9. D.H. Tsai and C.W. Beckett, "Shock Wave Propagation in Cubic Lattices", J. Geophys. Res. 71, 2601 (1966).
10. D.H. Tsai and R.A. MacDonald, "Second Sound in a Solid Under Shock Compression", J. Phys. C 6, L171 (1973).
11. J.C. Ward and J. Wilks, "Second Sound and the Thermo-Mechanical Effect at Very Low Temperatures", Phil. Mag. 43, 48 (1952).
12. M. Chester, "Second Sound in Solids", Phys. Rev. 131, 2013 (1963).

pretation. First, current theories of second sound suggest that it can only occur under extremely limited experimental conditions. Specifically, the temperature must be sufficiently low that umklapp phonon scattering processes[13] are negligible, but sufficiently high that normal processes have been activated. Unless the first condition is satisfied, the second-sound wave is rapidly damped in time, and, unless the second condition is met, only ballistic propagation occurs. It is difficult to see how such conditions can be met in a crystal under shock compression where one would ordinarily expect umklapp scattering to be of utmost importance. Second, although the propagation into the crystal of a thermally equilibrated region behind the shock front is superficially similar to the propagation of a second-sound wave, we view these processes to be fundamentally different physical phenomena. In the shock-wave case, directed energy which is deposited into the crystal by the shock front relaxes to thermal equilibrium behind the front; if the relaxation time is constant, the thermally equilibrated part of the crystal will clearly propagate at the speed of the front and the profile will be steady in time. In the second-sound case, thermal or "random" energy propagates into the crystal. Ordinarily this energy propagates only by diffusion but, under the limited experimental conditions discussed above, it can propagate at the higher speed of second sound. In our view, then, in order to explain the nonsteady behavior of the shock profile, it is necessary to explain why the relaxation time increases with increasing distance into the crystal.

We should also point out that two additional conclusions of Tsai's work contradict continuum theories of shock propagation. First, the energy density immediately behind the front appears to substantially overshoot its final equilibrated value. To our knowledge, no detailed explanation of this effect has been offered. Second, the Hugoniot conditions, which relate the initial and final values of the pressure, density, energy, and velocity are not identically satisfied. The lack of agreement has been attributed to the nonsteady behavior and this explanation seems reasonable in view of the fact that these conditions, in their usual form, are based on the assumption of steady state.

The only additional computer simulations of shock propagation in the three-dimensional lattice with which we are aware are the work of

13. J.M. Ziman, Electrons and Phonons (Oxford University Press, London, 1960), Chap. III.

Paskin and his coworkers[14,15]. These investigations have been considerably less extensive than those of Tsai. It is difficult to conclude from their results whether the profile is steady since the shock wave has been allowed to propagate only a short distance into the lattice. The Hugoniot conditions were checked and reported to be satisfied. Although this conclusion appears to contradict the work of Tsai, we should point out that Tsai found deviations of only a few percent and, since the results are highly dependent upon very accurate determination of the thermodynamic variables under consideration, the question must be considered unsettled.

In addition to the work on three-dimensional crystals, shock propagation in one-dimensional chains has also been under active investigation. Manvi, Duvall, and coworkers[16-18], in an effort to resolve some of the more puzzling questions, have studied the problem in detail. They, too, observed a nonsteady profile and found that no temperature rise existed behind the front. Computer solution of the atomic equations of motion for a one-dimensional, weakly anharmonic chain have also been undertaken by Tasi[19-21]. The numerical solutions were then verified by an elegant perturbation technique. Tasi's results were in essential agreement with those of Manvi et al. In addition, the shock wave was allowed to propagate considerably farther into the lattice than in previous investigations. At distances far into the lattice, the propagation of well-defined, stable pulses (solitary waves) was found in the vicinity of the shock front. In Tasi's work as well

14. A. Paskin and G.J. Dienes, "Molecular Dynamic Simulations of Shock Waves in a Three-Dimensional Solid", J. Appl. Phys. 43, 1605 (1972).
15. A. Paskin and G.J. Dienes, "A Model for Shock Waves in Solids and Evidence for a Thermal Catastrophe", Solid State Comm. 17, 197 (1975).
16. R. Manvi, G.E. Duvall, and S.C. Lowell, "Finite Amplitude Longitudinal Waves in Lattices", Int. J. Mech. Sci. 11, 1 (1969).
17. G.E. Duvall, R. Manvi, and S.C. Lowell, "Steady Shock Profile in a One-Dimensional Lattice", J. Appl. Phys. 40, 3771 (1969).
18. R. Manvi and G.E. Duvall, "Shock Waves in a One-Dimensional, Non-Dissipating Lattice", Brit. J. Appl. Phys. 2, 1389 (1969).
19. J. Tasi, "Perturbation Solution for Growth of Nonlinear Shock Waves in a Lattice", J. Appl. Phys. 43, 4016 (1972). See also Erratum (J. Appl. Phys. 44, 1414, (1973)).
20. J. Tasi, "Far-Field Analysis of Nonlinear Shock Waves in a Lattice", J. Appl. Phys. 44, 4569 (1973).
21. J. Tasi, "Perturbation Solution for Shock Waves in a Dissipative Lattice", J. Appl. Phys. 44, 2245 (1973).

as that of Manvi and his coworkers, it was assumed that the atoms of the crystal were initially at rest in their equilibrium positions prior to excitation by the shock wave. Thus, the seemingly important effect on shock propagation of a nonzero ambient temperature was not examined in these one-dimensional calculations.

These questions will be addressed in considerably greater detail in the text of this report in which we describe the results of calculations undertaken using our own computer program written in-house. To summarize, our motivation for this work has been as follows: Shock-wave studies in three-dimensional crystals have raised, but in our opinion failed to answer, a number of important questions, particularly regarding the existence of steady state and the approach to thermal equilibrium. Attempts to answer these questions using simpler one-dimensional models have been excellent, but largely inconclusive. In view of the importance of understanding shock propagation to Army-related problems, it was considered worthwhile to develop our own in-house capability for studying these problems. The one-dimensional code discussed here is an initial step in the writing of a more complicated three-dimensional code which we plan to undertake in the near future.

The organization of the report is as follows: In Sec. 2, we indicate the model as well as discuss the interatomic potentials used in our calculations. In Sec. 3, an exact analytic solution for the propagation of compression waves in the harmonic, one-dimensional lattice is presented. In Sec. 4, the equations of motion are rewritten in nondimensional form and the numerical method employed in the computer code discussed. Section 5 contains the results of the numerical solution of the equations of motion for the anharmonic lattice. Prior to excitation by the shock, the atoms were initially at rest in their equilibrium positions. Solitary waves are found to propagate in the vicinity of the front and an analytic approximation for the shape of the solitary waves is presented. In Sec. 6, the results of Sec. 5 are extended to the case in which the lattice is characterized by some nonzero initial temperature. Considerable discussion of the results is given in each section. Section 7 contains a summary and conclusion as well as our intentions for future work.

2. MODEL AND INTERATOMIC POTENTIALS

The model under consideration for the present calculations consists of a one-dimensional chain of atoms, each having mass m, which interact through some interatomic potential to be specified. (See Fig. 1.) The total number of atoms in the chain is N and the equilibrium spacing between successive atoms is a_0. The coordinate x_j represents the displacement of the j^{th} atom from its equilibrium postion, r_j is the distance to the j^{th} atom from a common origin

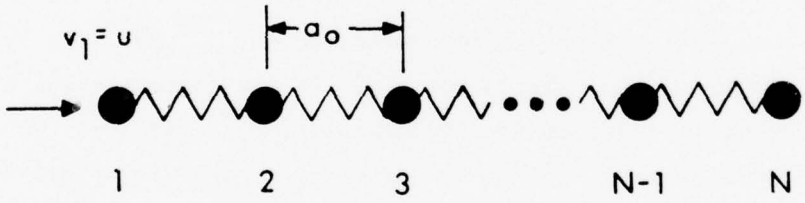

Figure 1. Model for simulating shock propagation in a one-dimensional, discrete lattice.

(chosen to be the equilibrium position of the first atom), and r_{0j} is the corresponding distance to the equilibrium site of the j^{th} atom. The coordinates are related by the expression

$$r_j = r_{0j} + x_j \ . \tag{2.1}$$

The purpose of the calculation then is to solve the classical equations of motion of the atoms when the first atom is subjected to steady compression at velocity u.

The Hamiltonian for the chain can be written as

$$H = \tfrac{1}{2} m \sum_{j=1}^{N} v_j^2 + \Phi (r_1, r_2, \ldots r_N) \tag{2.2}$$

where $v_j = dx_j/dt$ is the velocity of the j^{th} particle and Φ is the total potential energy of the lattice. The differential equation of motion of the j^{th} particle is then clearly

$$m \frac{d^2 x_j}{dt^2} = F_j + F_j^{ext} \tag{2.3}$$

where $F_j = - \partial\Phi/\partial x_j$ is the force exerted on the j^{th} particle by the remaining atoms of the lattice and F_j^{ext} is the corresponding external force. For the problem under consideration, F_j^{ext} is zero for all particles except the first and then it is $-F_1$ since this particle moves at constant velocity u.

If we assume that the atoms undergo only small deviations from their equilibrium positions, the potential Φ can be expanded in a Taylor series about the atoms' equilibrium positions such that

$$\Phi = \Phi_0 (r_{01}, r_{02}, \ldots r_{0N}) + \tfrac{1}{2} \sum_{i,j=1}^{N} \phi_{ij} x_i x_j \tag{2.4}$$

where Φ_0 is a constant which will arbitrarily be set equal to zero hereafter and where

$$\phi_{ij} = \left(\frac{\partial^2 \Phi}{\partial r_i \partial r_j} \right)_{r_{0i}, r_{0j}} \ . \tag{2.5}$$

The first-derivative term in the Taylor expansion for the potential vanishes since the expansion is about the equilibrium positions of the atoms. The potential represented by Eq. (2.4) is the so-called harmonic potential. Finally, if we assume only nearest-neighbor interactions such that only the $j + 1^{st}$ and $j - 1^{st}$ atom exert an appreciable force on the j^{th} atom, we have

$$\phi_{ij} = - \gamma \, (\delta_{i,j-1} - 2 \, \delta_{ij} + \delta_{i,j+1}) \tag{2.6}$$

where γ is the force constant of the "spring" connecting successive particles and δ is the Kronecker δ. Equations (2.3) - (2.6) then imply that the equation of motion of the j^{th} particle is given in the harmonic approximation by

$$m \frac{d^2 x_j}{dt^2} = \gamma \, (x_{j+1} - 2x_j + x_{j-1}) + F_j^{ext} \quad . \tag{2.7}$$

Equation (2.7) is a linear, second-order, differential equation and, as we shall see in the following section, it is amenable to exact analytic solution.

Particularly at low temperatures, the harmonic approximation to the interatomic potential is usually adequate for calculating most equilibrium properties of the lattice. For several reasons, however, the approximation is generally inadequate for the study of the shock-wave problem. First, at the high temperatures present in most shock-wave calculations, the atoms undergo substantial deviations from their equilibrium positions and the Taylor expansion represented in Eq. (2.4) is no longer valid. Second, if one performs a normal-mode analysis to solve analytically the equations of motion for a system of coupled harmonic oscillators, it is found that the energy of each mode is a constant of the motion. Consequently, there exists no mechanism in the harmonic approximation for redistributing the energy among the various modes. This system then, if disturbed from thermal equilibrium, can never return to equilibrium. Finally, it is known that anharmonic terms are responsible for the steepening effect which forms a shock wave from the initial compression of the lattice. Any realistic lattice-dynamical study of shock propagation must, therefore, be based upon a model which includes anharmonic interactions.

Two anharmonic potentials which have been widely used in lattice-dynamical calculations, and in particular in the study of shock-wave phenomena, are the Morse and Lennard-Jones potentials. These potentials are semi-empirical and based on the assumption that only two-body interactions are important. If we further restrict consideration to only nearest-neighbor interactions the potentials can be written,

respectively, as

$$\Phi_M = D \sum_{i=2}^{N} \left[e^{-\alpha(x_i - x_{i-1})} - 1 \right]^2 \tag{2.8}$$

and

$$\Phi_{LJ} = \varepsilon \sum_{i=2}^{N} \left[\frac{a_0^6}{(a_0 + x_i - x_{i-1})^6} - 1 \right]^2 . \tag{2.9}$$

In these expressions, ε,D, and α are constants which are usually fit to the experimental data. That the potentials are qualitatively similar has been shown, for instance, by Choquard[22]. Since it is slightly easier to treat numerically, we will confine our attention in the remainder of this report to only the Morse potential.

One additional potential which will be discussed only briefly in the text of this report is the so-called hard-sphere interaction first suggested by Northcote and Potts[23] in their study of the Fermi-Pasta-Ulam problem. In this approximation, it is assumed that the atoms of the chain can be represented by hard spheres of diameter d connected by harmonic springs. Between collisions, the motion of the atoms is governed by the harmonic approximation. Whenever the atomic separation of successive atoms becomes equal to d, however, the atoms undergo an elastic collision in which their momenta are interchanged. For reasons discussed in Sec. 5, it is of interest to study this interaction briefly.

22. P. Choquard, The Anharmonic Crystal (Benjamin, New York, 1967), Chap. 6.
23. R.S. Northcote and R.B. Potts, "Energy Sharing and Equilibrium for Nonlinear Systems", J. Math. Phys. 5, 383 (1964).

3. THE HARMONIC LATTICE

Propagation of compression pulses in one-dimensional, harmonic chains has been extensively studied[24-28]. For reasons discussed in the previous section, a harmonic lattice cannot support a shock wave in the usual sense. Nevertheless, it is interesting to carry out the calculation since the result lends physical insight into the calculation for the anharmonic case, and also provides a useful limiting-case check for the numerical calculations undertaken subsequently.

The first detailed solution of this problem was apparently given by Schroedinger[29] who noted that the equations of motion for the atoms could be put in a form that resembled the recursion relation for Bessel functions of the first kind. In this section we shall present a more detailed calculation, involving a normal-mode analysis, which we believe is somewhat more illustrative of the physical principles involved.

We shall begin by solving the atomic equations of motion for the atoms of an infinite, one-dimensional, harmonic lattice for arbitrary initial conditions. The atoms are distributed symmetrically about the zeroth atom, which is located at the origin (See Fig. 2). No external forces act on the chain. We then show that by judiciously choosing the initial velocities and positions of the particles for $j \leq 1$, the first particle can be made to travel to the right at a constant velocity u for all time. In other words, the boundary-value problem corresponding to shock propagation in a semi-infinite lattice can be transformed to an initial-value problem for an infinite chain. We then use this model to investigate the shock profile for two sets of initial conditions. In the first case, the particles for which $j > 1$ are assumed to be initially at rest in their equilibrium positions, whereas, in the second calculation, their velocities are distributed according to a Maxwellian distribution at temperature T.

---

24. P.M. Morse and K.U. Ingard, Theoretical Acoustics (McGraw-Hill, New York, 1968), Chap. 3.
25. R. Weinstock, "Propagation of a Longitudinal Disturbance on a One-Dimensional Lattice", Am. J. Phys. 38, 1289 (1970).
26. E.M. Baroody and E. Drauglis, "Propagation of a Sharp Disturbance Along a One-Dimensional Lattice", Am. J. Phys. 39, 1412 (1971).
27. A.H. Nayfeh and M.H. Rice, "On The Propagation of Disturbances in a Semi-Infinite One-Dimensional Lattice", Am. J. Phys. 40, 469 (1972).
28. F.O. Goodman, "Propagation of a Disturbance on a One-Dimensional Lattice Solved by Response Functions", Am. J. Phys. 40, 92 (1972).
29. E. Schroedinger, "Zur Dynamik Elastisch Gekoppelter Punktsysteme", Ann. Phys. 44, 916 (1914).

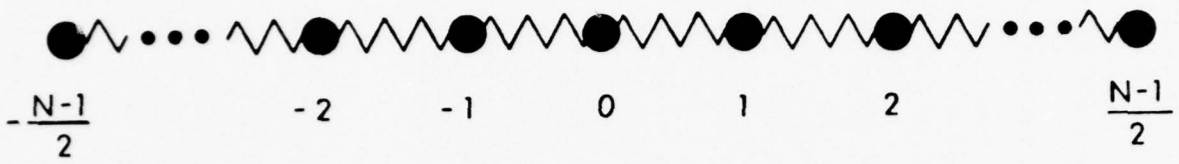

Figure 2. Model for solving the equations of motion for a one-dimensional, harmonic lattice. For convenience, N is chosen to be odd.

3.1 General Solution of the Equations of Motion for the Infinite, One-Dimensional, Harmonic Chain

Consider a chain consisting of N atoms connected by harmonic springs of force constant γ. Every atom has mass m and is labeled by index j such that

$$-\frac{N-1}{2} \leq j \leq \frac{N-1}{2} \quad .$$

We assume for convenience that N is odd. It will be made arbitrarily large in the final results.

The differential equation of motion for the j^{th} atom, assuming only nearest-neighbor interactions, is given by Eq. (2.7) without the forcing term, viz.,

$$m \frac{d^2 x_j}{dt^2} = \gamma \left(x_{j+1} - 2 x_j + x_{j-1}\right) \quad . \tag{3.1}$$

Since we anticipate oscillatory solutions of this equation, we assume a solution of the form

$$x_j = C_j \, e^{i(\omega t + \delta)} \quad , \tag{3.2}$$

where C_j is the amplitude, ω is the frequency, and δ is a phase factor. The real part of Eq. (3.2) is, of course, implied. Substitution of Eq. (3.2) into (3.1) yields for the eigenvectors C_j the relation

$$-m\omega^2 C_j = \gamma \left(C_{j+1} - 2 C_j + C_{j-1}\right) \quad . \tag{3.3}$$

Considerable simplification in the solution of Eq. (3.3) arises if we assume periodic boundary conditions such that

$$C_j = C_{j+N} \quad . \tag{3.4}$$

As N is made arbitrarily large, the boundary conditions at the ends of the chain are insignificant. To solve Eq. (3.3), let

$$C_j = z^j \quad , \tag{3.5}$$

which upon substitution into Eq. (3.4) yields

$$z^N = 1$$

or

$$z = e^{2\pi i s'/N}, \quad s' = \frac{-N+1}{2}, \frac{-N+3}{2}, \ldots \frac{N-1}{2} \tag{3.6}$$

or

$$z = e^{isa_0} \quad . \tag{3.7}$$

Here,

$$s = \frac{2\pi s'}{L} \tag{3.8}$$

where $L=Na_0$ is the total length of the chain and a_0 is the equilibrium spacing. Finally, from Eqs. (3.7) and (3.5) we have

$$C_j^s = e^{ijsa_0} \quad . \tag{3.9}$$

The superscript s has been added to denote that C_j is the eigenvector associated with a particular one of the N values of s.

If the solution represented by Eq. (3.9) is substituted into the original expression, Eq. (3.3), we obtain after some algebra the result

$$\omega_s = \omega_0 \left|\sin(sa_0/2)\right| , \tag{3.10}$$

where

$$\omega_0 = \sqrt{4\gamma/m}. \tag{3.11}$$

The frequencies represented by Eq. (3.10) are the N normal-mode frequencies in which the lattice can oscillate. The speed v_s with which a particular normal mode, characterized by frequency ω_s, propagates is given by the relation

$$v_s = \frac{\partial\omega_s}{\partial s} = \frac{\omega_0 a_0}{2} \left|\cos(sa_0/2)\right| \quad . \tag{3.12}$$

The low-frequency, long-wavelength modes, characterized by small values of s, propagate at a velocity nearly equal to $\omega_0 a_0/2$ which is just the ordinary sound speed in the crystal. The higher-frequency modes, however, propagate more slowly and, thus, the lattice exhibits dispersion.

The solution represented by Eq. (3.2) is only a particular solution for x_j. In general, in order to satisfy the initial conditions, x_j must be expanded in terms of the complete set of eigenvectors C_j^s. Thus we have

$$x_j = 1/2 \sum_s \left[n_s C_j^s e^{i(\omega_s t+\delta_s)} + n_s^* C_j^{*s} e^{-i(\omega_s t+\delta_s)} \right] \qquad (3.13)$$

where the real part has been taken explicitly and where the asterisks denote complex conjugates. The quantities n_s and δ_s are to be determined from the initial conditions.

Let a_j and $\dot{a}_j$ represent the values of x_j and dx_j/dt at time $t=0$. Substitution into Eq. (3.13) then yields

$$a_j = 1/2 \sum_s \left[n_s C_j^s e^{i\delta_s} + n_s^* C_j^{*s} e^{-i\delta_s} \right]$$

and (3.14)

$$\dot{a}_j = \frac{i}{2} \sum_s \left[n_s \omega_s C_j^s e^{i\delta_s} - n_s^* \omega_s C_j^{*s} e^{-i\delta_s} \right] .$$

If Eqs. (3.14) are multiplied by C_j^{*s} and summed over j, one finds with the help of the orthogonality relation

$$\sum_j C_j^s C_j^{*s'} = N\delta_{ss'} \qquad (3.15)$$

that

$$n_s e^{i\delta_s} = \frac{1}{N} \sum_j \left(a_j - \frac{i\dot{a}_j}{\omega_s} \right) C_j^{*s} \quad . \qquad (3.16)$$

Substitution of Eq. (3.16) into Eq. (3.13) then yields

$$x_j = \frac{1}{N} \sum_{s,k} \left\{ a_k \cos \left[(j-k)\, s\alpha_0 + \omega_s t \right] + \frac{\dot{a}_k}{\omega_s} \sin \left[(j-k) s\alpha_0 + \omega_s t \right] \right\} . \qquad (3.17)$$

In obtaining this result, we have used Eq. (3.9).

Equation (3.17) represents the general solution of the equation of motion for the displacement of the j^{th} atom in terms of the initial conditions of all the particles in the chain. The velocity can, of course, be obtained by differentiation with respect to t. As N becomes arbitrarily large, the right-hand side of Eq. (3.17) changes negligibly as s assumes successive values and the sum over s can be replaced by an integral. Examination of Eqs. (3.6) and (3.8) shows that this replacement is effected by using the prescription

$$\sum_s \to \frac{L}{2\pi} \int_{-\pi/a_0}^{\pi/a_0} ds \quad .$$

The region of s space contained between $\pm \pi/a_0$ is known as the first Brillouin zone. Thus Eq. (3.17) becomes

$$x_j = \frac{a_0}{2\pi} \sum_{k=-\infty}^{\infty} \int_{-\pi/a_0}^{\pi/a_0} ds \left\{ a_k \cos \left[(j-k)sa_0 + \omega_s t\right] + \frac{\dot{a}_k}{\omega_s} \sin \left[(j-k)\, sa_0 + \omega_s t\right] \right\} \quad . \tag{3.18}$$

It remains only to evaluate the integral appearing in Eq. (3.18). To do so, we make the change of variable

$$y = \frac{sa_0}{2} \quad .$$

Some rearrangement of Eq. (3.18) then yields the equivalent expression

$$x_j = \frac{2}{\pi} \sum_k \int_0^{\pi/2} dy \left\{ a_k \cos \left[2(j-k)y\right] \cos(\omega_0 t \sin y) + \frac{\dot{a}_k}{\omega_0 \sin y} \cos \left[2(j-k)y\right] \sin(\omega_0 t \sin y) \right\} \quad . \tag{3.19}$$

We have used Eq. (3.10) to express ω_s in terms of y. We now make use of the generating functions[30]

$$\cos(z \sin\theta) = J_0(z) + 2\sum_{k=1}^{\infty} J_{2k}(z)\cos(2k\theta)$$
$$\sin(z \sin\theta) = 2\sum_{k=0}^{\infty} J_{2k+1}(z)\sin[(2k+1)\theta] \tag{3.20}$$

where J_ℓ is the Bessel function of the first kind of order ℓ. Use of Eq. (3.20) in (3.19) allows immediate evaluation of the y integration. Ultimately, the result becomes

$$x_j(t) = \sum_{k=-\infty}^{\infty}\left[a_k J_{2j-2k}(\omega_0 t) + \frac{2\dot{a}_k}{\omega_0}\sum_{m=j-k}^{\infty} J_{2m+1}(\omega_0 t)\right] . \tag{3.21}$$

The velocity of the j^{th} particle can be obtained by time differentiation of Eq. (3.21). Noting that[30]

$$\frac{dJ_n(z)}{dz} = 1/2\left[J_{n-1}(z) - J_{n+1}(z)\right] \tag{3.22}$$

allows us, after some manipulation, to write the result in the form

$$v_j(t) = \sum_{k=-\infty}^{\infty}\left[\dot{a}_k J_{2j-2k}(\omega_0 t) + \frac{\omega_0}{2}(a_k - a_{k+1}) J_{2j-2k-1}(\omega_0 t)\right] . \tag{3.23}$$

Equations (3.21)and (3.23), which represent a general solution to the equations of motion for the j^{th} particle in the harmonic chain, are the central result of this subsection. In the following subsection they are applied to the shock-wave problem.

30. Handbook of Mathematical Functions, edited by M. Abramowitz and I. Stegun (Natl. Bur. Std., Washington, DC, 1964), Chap. 9.

3.2 Application to Shock-Wave Problem

In order to apply the solution for the infinite chain to the shock-wave case, we must generate the following set of initial conditions: (1) The initial displacements and velocities to the left of the first particle, which are at our disposal, must be chosen so that the first particle moves at constant speed u for all t. (2) The initial displacement of the first particle is zero and its initial velocity is u. (3) The initial conditions for particles to the right of the first particle are arbitrary. Under these conditions, the steady compression of the first particle will generate a shock wave in the right-most part of the lattice.

The symmetry of the problem suggests that we examine the following initial conditions for the particles to the left of the first particle in the chain

$$\begin{aligned} a_k &= -a_{-k+2} \\ \dot{a}_k &= 2u - \dot{a}_{-k+2} \quad . \end{aligned} \tag{3.24}$$

Note that these conditions imply $a_1 = 0$, $\dot{a}_1 = u$. If these initial conditions are substituted into Eqs. (3.21) and (3.23), we find after some tedious manipulation of the summation indices

$$\begin{aligned} x_j(t) = \frac{2u}{\omega_0} \sum_{k=0}^{\infty} (2k+1)\, J_{2j+2k-1}(\omega_0 t) \\ + \frac{2}{\omega_0} \sum_{k=2}^{\infty} \dot{a}_k \sum_{m=j-k}^{j+k-3} J_{2m+1}(\omega_0 t) \\ + \sum_{k=2}^{\infty} a_k \left[J_{2j-2k}(\omega_0 t) - J_{2j+2k-4}(\omega_0 t) \right] \end{aligned} \tag{3.25}$$

and

$$v_j(t) = u\, J_{2j-2} + \sum_{k=2}^{\infty} \Big\{ 2u\, J_{2j+2k-4}(\omega_0 t) + \dot{a}_k \left[J_{2j-2k}(\omega_0 t) - J_{2j+2k-4}(\omega_0 t) \right] - \frac{\omega_0}{2}\, a_k \left[J_{2j-2k+1}(\omega_0 t) - J_{2j-2k-1}(\omega_0 t) - J_{2j+2k-3}(\omega_0 t) + J_{2j+2k-5}(\omega_0 t) \right] \Big\} \quad . \tag{3.26}$$

For the first particle in the chain, we substitute j=1 in Eqs. (3.25) and (3.26) and obtain the result

$$x_1(t) = ut \tag{3.27}$$

$$v_1(t) = u \tag{3.28}$$

for all t. In obtaining Eqs. (3.27) and (3.28) we have made use of the following relations for Bessel functions[30]:

$$J_{-n}(x) = (-1)^n J_n(x) \tag{3.29}$$

$$J_0(x) + 2 \sum_{k=1}^{\infty} J_{2k}(x) = 1 \tag{3.30}$$

and

$$2 \sum_{k=0}^{\infty} (2k+1)\, J_{2k+1}(x) = x \quad . \tag{3.31}$$

Thus, the initial conditions suggested in Eq. (3.24) give rise to steady motion of the first particle to the right at velocity u. Equations (3.25) and (3.26) represent the time-dependent velocity and displacement of the j^{th} particle in response to the resulting shock wave. Our interest, of course, is only in particles to the right of j=0.

3.3 Propagation in the Initially Quiescent Lattice

Equations (3.25) and (3.26) can be greatly simplified if we assume that initially all particles to the right of the first are at rest in their equilibrium positions. Under this assumption, the equations become simply

$$x_j(t) = \frac{2u}{\omega_0} \sum_{k=0}^{\infty} (2k+1)\, J_{2j+2k-1}(\omega_0 t) \tag{3.32}$$

and

$$v_j(t) = u\, J_{2j-2}(\omega_0 t) + 2u \sum_{k=2}^{\infty} J_{2j+2k-4}(\omega_0 t) \quad . \tag{3.33}$$

The infinite series in Eqs. (3.32) and (3.33) converge rapidly and evaluation of the sums poses no major difficulty. We have written a short computer program which performs the calculation and we now turn to a discussion of the results.

In Fig. 3, we have plotted the nondimensionalized velocity of each particle given by

$$V_j = v_j/u \tag{3.34}$$

as a function of particle number, j. Results are presented for two different values of the nondimensionalized time

$$\tau = \omega_0 t \ . \tag{3.35}$$

From the results it is clear that the shock front propagates at the rate of approximately one-half particle per unit of nondimensional time τ. This result could have been anticipated from Eq. (3.12), which indicates that the maximum normal-mode velocity is one-half lattice spacing per unit of nondimensional time. The most important conclusion that can be drawn from the figure is that the shock profile is not steady in time. Rather, behind the front, there exists a region of oscillation with each particle oscillating about a mean value of u, the compression velocity. The extent of the region of oscillation increases with increasing distance into the lattice and is indicative of the dispersive character of the lattice discussed previously. Since the higher-frequency components of the compression will continue to trail farther behind the head of the front, we conclude that the region of oscillations must continue to grow.

In Fig. 4, we have shown the velocity-time trajectories of two typical particles in the lattice. Prior to excitation by the shock front, the 100^{th} particle is at rest in its equilibrium position. Upon

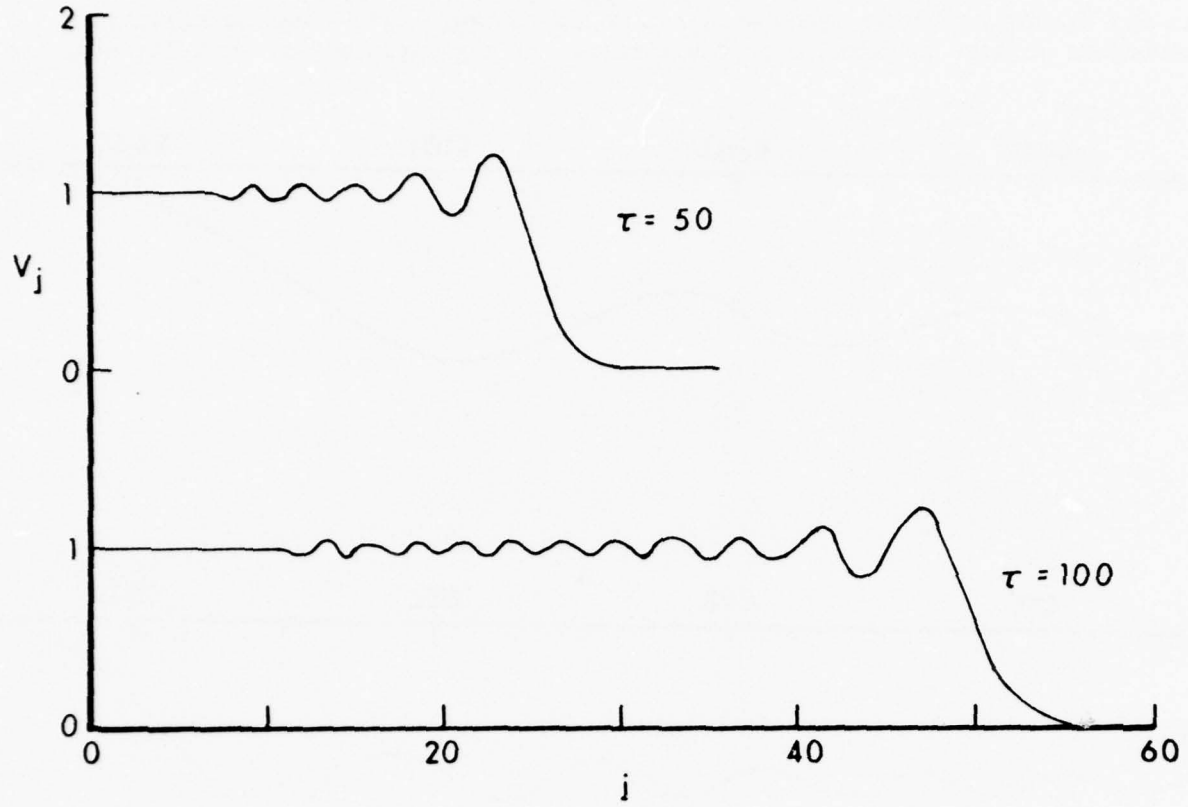

Figure 3. Nondimensional velocity as a function of particle number in the harmonic lattice.

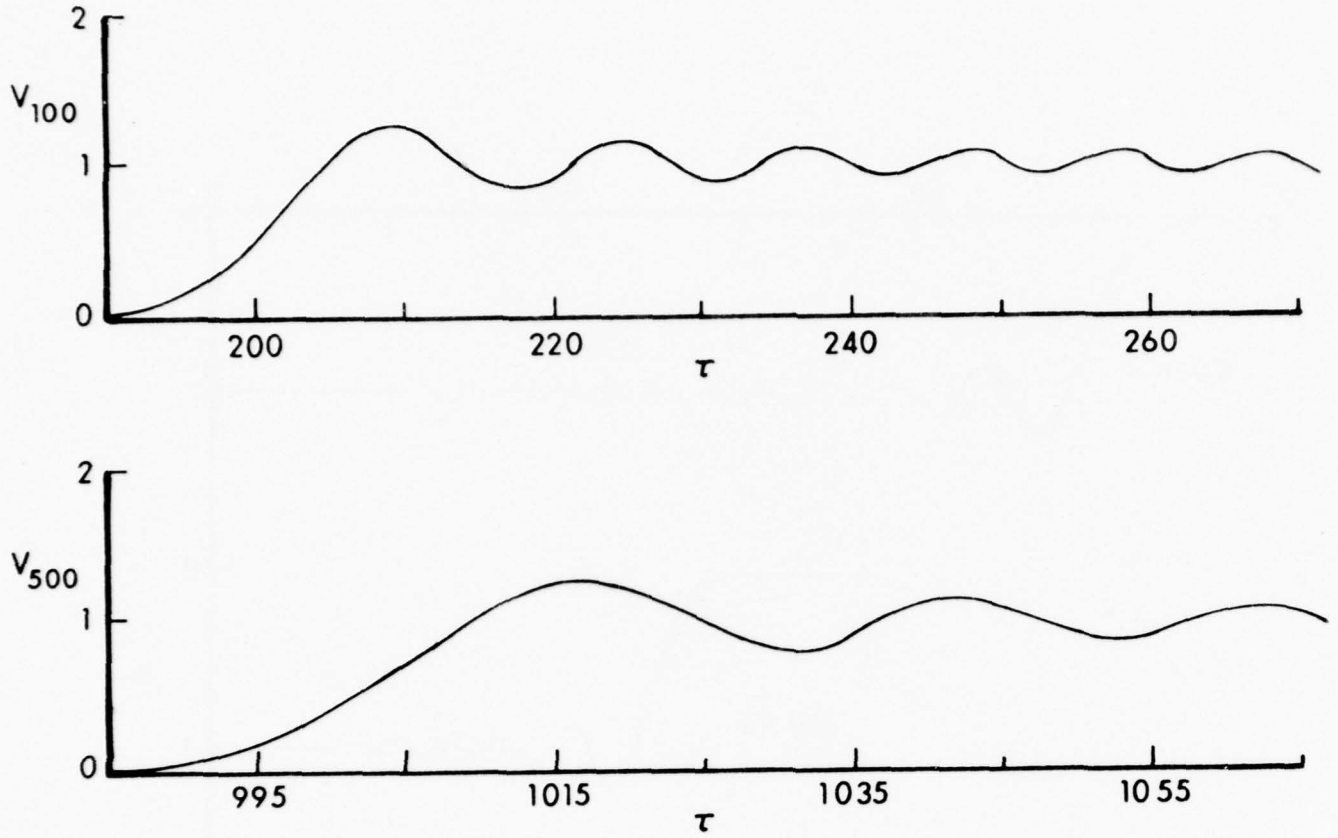

Figure 4. Velocity-time trajectories for two particles in the harmonic lattice subsequent to excitation by the shock. The origin of the time scale is approximately the time at which the particle first feels the effect of the front.

excitation, it reaches a maximum nondimensional velocity of about 1.25, and then oscillates with decaying amplitude about unity. A similar effect is observed for the 500^{th} particle in the lattice, except that the decay time for the velocity is longer than for the 100^{th} particle, again because of dispersion.

Well behind the shock front, all particles are observed to move uniformly at the compression velocity; consequently there is no temperature rise behind the shock front. This effect is not unexpected because, as pointed out earlier, there is no mechanism in the harmonic lattice for "randomizing" the energy deposited in the lattice by the shock wave. That the velocities behind the front should eventually approach the compression velocity can be seen directly from the asymptotic expansion (large t) of Eq. (3.33). For ν fixed and finite, one has[30]

$$\lim_{z\to\infty} J_\nu(z) = 0 \quad . \tag{3.36}$$

In Eq. (3.33), let $j+k=\ell$. Some rearrangement of the equation then yields the equivalent expression

$$v_j(t) = u\, J_{2j-2}(\omega_0 t) + 2u \sum_{\ell=3}^{\infty} J_{2\ell-4}(\omega_0 t) - 2u \sum_{\ell=3}^{j+1} J_{2\ell-4}(\omega_0 t) \quad . \tag{3.37}$$

Equations (3.30) and (3.36) then imply

$$\lim_{\substack{t\to\infty \\ j \text{ finite}}} v_j(t) = u \quad . \tag{3.38}$$

3.4 Effect of Nonzero Initial Conditions

In the preceding subsection we have obtained a solution of the atomic equations of motion for the shock-compressed chain under the assumption that the atoms were initially at rest in their equilibrium positions. Different microscopic initial conditions will lead to different results, of course, and it is of interest to ask if an average taken over a large set of such initial conditions will lead to a steady profile.

To examine this question, consider an ensemble of initial conditions in which the particles in the right-most part of the chain are in their equilibrium positions, but their velocities are characterized by a Maxwellian distribution at temperature T. These initial conditions are summarized by the initial distribution function

$$F(0) = \frac{1}{Z} \prod_{j=2}^{\infty} \exp \left[- m \dot{a}_j^2 / (2kT) \right] \tag{3.39}$$

where k is Boltzmann's constant and Z is the partition function which normalizes the distribution to unity. The ensemble average of $x_j(t)$ and $v_j(t)$ is then obtained by multiplying Eqs. (3.25) and (3.26) (with all a_k set equal to zero) by Eq. (3.39) and evaluating the integral over phase space.

For the velocity, we obtain the result

$$\begin{aligned} \langle v_j(t) \rangle = \frac{1}{Z} \int_{-\infty}^{\infty} d\dot{a}_2 \int_{-\infty}^{\infty} d\dot{a}_3 \cdots \Bigg\{ & u J_{2j-2}(\omega_0 t) \\ & + \sum_{k=2}^{\infty} \left[2u J_{2j+2k-4}(\omega_0 t) + \dot{a}_k J_{2j-2k}(\omega_0 t) \right. \\ & \left. - \dot{a}_k J_{2j+2k-4}(\omega_0 t) \right] \Bigg\} \prod_{j=2}^{\infty} \exp \left[-m \dot{a}_j^2 / (2kT) \right] \end{aligned} \tag{3.40}$$

where the brackets denote ensemble average. The integrals over the $\dot{a}_k$ vanish because of the antisymmetry of the integrand, leaving

$$\begin{aligned} \langle v_j(t) \rangle = & \left[u J_{2j-2}(\omega_0 t) + 2u \sum_{k=2}^{\infty} J_{2j+2k-4}(\omega_0 t) \right] \\ & \times \frac{1}{Z} \int_{-\infty}^{\infty} d\dot{a}_2 \int_{-\infty}^{\infty} d\dot{a}_3 \cdots \prod_{j=2}^{\infty} \exp \left[- m \dot{a}_j^2 / (2kT) \right] . \end{aligned} \tag{3.41}$$

The remaining integration in Eq. (3.41) is just the definition of the partition function. Consequently, we again obtain the result of Eq. (3.33). A similar result holds for the ensemble average of the displacement, $x_j(t)$.

We conclude that an average taken over many experiments in which the initial conditions are characterized by Eq. (3.39) will lead to the same results for the (average) velocity and displacement as for the case in which the initial conditions are zero. In essence, averaging the initial conditions and then doing an experiment is equivalent to averaging the results of many experiments with different initial conditions. This is certainly not true in general and results from the fact that the solutions of the equations of motion depend only linearly on the initial values of the velocity and displacement.

4. NONDIMENSIONALIZED EQUATIONS AND METHOD FOR SOLUTION

The equations of motion for the atoms of a one-dimensional, harmonic lattice can be solved analytically, as has been shown in the last section. For the case in which anharmonic terms are present, however, one must resort to numerical techniques. In this section, we consider the differential equation of motion for the j^{th} particle when the interatomic potential is the Morse potential represented by Eq. (2.8). We define certain nondimensional quantities and write the equations in terms of these quantities. The numerical technique used in the computer solution of these equations is then discussed. Finally, the mechanics of the computer code and the actual quantities calculated are indicated briefly.

Consider the Morse potential in Eq. (2.8) which represents the interatomic interaction between nearest-neightbor particles in the lattice. As the values of x_i become small, the exponential term can be expanded to produce, to lowest order,

$$\Phi_m \sim D\,a^2 \sum_{i=2}^{N} (x_i - x_{i-1})^2 , \tag{4.1}$$

which is, of course, just the harmonic limit of this interaction. We can, therefore, equate the constant Da^2 to one-half the harmonic force constant, γ. Use of Eq. (3.11) then implies

$$D = \frac{m\omega_0^2}{8a^2} \tag{4.2}$$

where ω_0 is, again, the maximum normal-mode frequency of the corresponding harmonic lattice. The total potential energy of the lattice can then be written

$$\Phi_M = \frac{m\omega_0^2}{8a^2} \sum_{i=2}^{N} \left\{ \exp\left[- a(x_i - x_{i-1}) \right] - 1 \right\}^2 \qquad (4.3)$$

where we have used Eqs. (2.8) and (4.2). In the absence of external forces, the differential equation of motion of the j^{th} particle is just given by the result

$$m \frac{d^2 x_j}{dt^2} = \frac{-\partial \Phi_m}{\partial x_j} = \frac{m\omega_0^2}{4a} \left\{ \exp\left[- 2a(x_j - x_{j-1}) \right] - \exp\left[-a(x_j - x_{j-1}) \right] \right.$$

$$\left. - \exp\left[- 2a(x_{j+1} - x_j) \right] + \exp\left[-a(x_{j+1} - x_j) \right] \right\} \qquad (4.4)$$

where the right-hand side has been obtained by differentiation of Eq. (4.3) with respect to x_j. Since the above equation contains no external forces, it applies only for $j \geq 2$. The first particle which moves at constant velocity u for all time satisfies the equation of motion

$$\frac{d^2 x_1}{dt^2} = 0 \qquad (4.5)$$

with initial conditions $x_1 = 0$, $dx_1/dt = u$.

Equations (4.4) and (4.5) constitute a set of N, coupled, nonlinear, second-order differential equations which must be solved numerically for various values of the parameters under consideration. Before discussing the method of solution of these equations, it is most convenient to convert them to a set of first-order equations and to rewrite them in terms of certain nondimensional quantities. To do so, we define a nondimensional displacement of the j^{th} particle by

$$S_j = \frac{\omega_0}{u} x_j \ , \qquad (4.6)$$

and a nondimensional time, τ, by the relation

$$\tau = \omega_0 t. \qquad (4.7)$$

The nondimensional velocity of the j^{th} particle is then given by

$$V_j = \frac{dS_j}{d\tau} = \frac{1}{u} \frac{dx_j}{dt} \qquad (4.8)$$

or simply the real velocity normalized by the compression velocity.

If we make use of Eqs. (4.6) - (4.8), we can cast Eqs. (4.4) and (4.5) in the form

$$\dot{S}_j = V_j$$

$$\dot{V}_j = \frac{1}{4A_m} \Big\{ \exp\left[-2A_m(S_j - S_{j-1})\right] - \exp\left[-A_m(S_j - S_{j-1})\right]$$

$$- \exp\left[-2A_m(S_{j+1} - S_j)\right] + \exp\left[-A_m(S_{j+1} - S_j)\right] \Big\} \quad j \geq 2$$

$$\dot{V}_1 = 0 \quad . \tag{4.9}$$

In these equations, A_m is given by the expression

$$A_m = \frac{au}{\omega_o} \tag{4.10}$$

and each dot represents differentiation with respect to the dimensionless time τ. The initial conditions of the first particle are given by $S_1 = 0$, $V_1 = 1$ and, for the remaining particles, the initial conditions depend upon the initial state of the lattice prior to compression. Note that the original N second-order equations have been converted to 2N first-order equations.

Most investigators have not employed this method of nondimensionalizing the equations of motion, but have used the lattice constant, a_0, to normalize the displacement. As a result, it is necessary that they supply two parameters as input data for their numerical calculations. The method which we have used requires specification of only one parameter, namely, A_m, to solve the equations and appears more convenient to use in the numerical calculations. It is interesting to point out that Manvi et al.[17] found it rather surprising that the solution of the equations of motion appeared to depend only on the product of the parameters a and u. The normalization adopted above, however, reveals that this must clearly be the case.

To solve Eq. (4.9) we employed a fourth-order Runge-Kutta scheme[31]. Given the values of the functions on the left-hand side of Eq. (4.9) at time τ, this method approximates their values at time $\tau + \Delta\tau$ by a

31. B. Carnahan, H.A. Luther, and J.O. Wilkes, Applied Numerical Methods (Wiley, New York, 1969), Chap. 6.

fourth-order polynomial in $\Delta\tau$. The 2N equations in Eq. (4.9) can be written in the general form

$$\frac{dy_j}{d\tau} = f_j(y_1, y_2, \ldots y_{2N}) \qquad j = 1,2,\ldots 2N \quad . \tag{4.11}$$

If $y_{j,i}$ represents the value of the function y_j at the beginning of the i^{th} time interval, its value at the end of the interval, $y_{j,i+1}$, is given by the following algorithm[31]:

$$y_{j,i+1} = y_{j,i} + \Delta\tau(k_{j1} + 2\,k_{j2} + 2\,k_{j3} + k_{j4})/6 \tag{4.12}$$

where

$$k_{j1} = f_j(y_{1,i}, y_{2,i}\cdots y_{2N,i}) \tag{4.12a}$$

$$y^*_{j,i} = y_{j,i} + 1/2\ \Delta\tau\ k_{j1} \tag{4.12b}$$

$$k_{j2} = f_j(y^*_{1,i}, y^*_{2,i}\cdots y^*_{2N,i}) \tag{4.12c}$$

$$\bar{y}_{j,i} = y_{j,i} + 1/2\ \Delta\tau\ k_{j2} \tag{4.12d}$$

$$k_{j3} = f_j(\bar{y}_{1,i}, \bar{y}_{2,i}\cdots \bar{y}_{2N,i}) \tag{4.12e}$$

$$\bar{y}^*_{j,i} = y_{j,i} + \Delta\tau\ k_{j3} \tag{4.12f}$$

$$k_{j4} = f_j(\bar{y}^*_{1,i}, \bar{y}^*_{2,i}\cdots \bar{y}^*_{2N,i}) \quad . \tag{4.12g}$$

The initial values of all functions are, of course, known and successive application of Eqs. (4.12) allows us to calculate them at any time τ.

We should mention that in our initial calculations, we did not use the Runge-Kutta method discussed above, but rather the improved Euler-Cauchy method[31] used by Tsai et al. and by Manvi et al. In this method, the value $y_{j,i+1}$ is approximated by a linear function of $\Delta\tau$, based on the value of the function and its slope at i. The slope at i+1 is then evaluated and an improved value of $y_{j,i+1}$ calculated from the average

of the slopes at i and i+1. The process is then repeated until successive iterations agree to within some prescribed tolerance. It is known, however, that this iterative technique is not so accurate as the fourth-order Runge-Kutta method[32] for the same value of $\Delta\tau$. In practice, we found that although a number of checks used to validate the computer code (discussed later in this section) were satisfied, varying the step size, $\Delta\tau$, led to completely different profiles when the Euler-Cauchy method was used. The effect became more and more pronounced as both τ and the nonlinearity parameter, A_m, increased. Some further discussion of this fact has been given by Manvi[33].

In addition to the velocities and displacements of each of the particles in the chain as a function of time, we have calculated in the program, a number of other quantities of interest such as the kinetic and potential energies of each particle and the force exerted on the N^{th} particle by the $N+1^{st}$. All energies have been nondimensionalized by the kinetic energy of the first particle, $1/2\ mu^2$, and all forces by the factor, $1/4\ m\omega_0 u$. The potential energy of a single particle was defined simply to be one-half of the potential energy of each of the "springs" to which the particle is attached. Thus, from Eq. (4.3), we have for the potential energy of the i^{th} particle,

$$\Phi_i = \frac{m\omega_0^2}{16a^2}\left(\left\{\exp\left[-a(x_i - x_{i-1})\right] - 1\right\}^2 + \left\{\exp\left[-a(x_{i+1} - x_i)\right] - 1\right\}^2\right). \tag{4.13}$$

This is not the only possible operational definition, but is a reasonable one.

In the remainder of this report, unless otherwise indicated, when we refer to the quantities discussed above we shall mean their nondimensionalized values. For reference, Table I indicates the quantity under consideration (column 1), the symbol for its nondimensional value (column 2), the normalizing factor by which the real quantity is divided to make it nondimensional (column 3), and the appropriate formula for the quantity of interest, where applicable (column 4).

32. A. Ralston, A First Course in Numerical Analysis (McGraw-Hill, New York, 1965), Chap. 5.
33. R. Manvi, "Shock Wave Propagation in a Dissipating Lattice Model", Ph.D. Thesis (Washington State University, 1968) (unpublished).

TABLE I. NONDIMENSIONAL PARAMETERS IN COMPUTER CALCULATION

REAL QUANTITY	SYMBOL FOR NONDIMENSIONALIZED VALUE	NORMALIZING FACTOR	FORMULA
Displacement of j^{th} particle	S_j	u/ω_o	
Velocity of j^{th} particle	V_j	u	
Kinetic energy of j^{th} particle	KE_j	$1/2\ m\ u^2$	$KE_j = V^2_j$
Potential energy of j^{th} particle	PE_j	$1/2\ m\ u^2$	$PE_j = \frac{1}{8A_m^2}\left(\left\{\exp\left[-A_m(S_j-S_{j-1})\right]-1\right\}^2 + \left\{\exp\left[-A_m(S_{j+1}-S_j)\right]-1\right\}^2\right)$
Force exerted on j^{th} particle by $j+1^{st}$	$F_{j,j+1}$	$1/4\ m\ \omega_0 u$	$F_{j,j+1} = \frac{1}{A_m}\left\{\exp\left[-A_m(S_{j+1}-S_j)\right] - \exp\left[-2A_m(S_{j+1}-S_j)\right]\right\}$

The remainder of this report will be concerned primarily with the numerical solution of Eq. (4.9) using the method just outlined. The results are discussed in the following two sections. We conclude this section by indicating a number of checks we used to insure the accuracy of our computational results.

First, we took the harmonic limit of Eq. (4.9) by expanding the exponentials and retaining only the first nonvanishing terms. The equations then become

$$\dot{S}_j = V_j$$

$$\dot{V}_j = 1/4(S_{j+1} - 2S_j + S_{j-1}) \qquad (4.14)$$

$$\dot{V}_1 = 0$$

with the same initial conditions as before. This set of equations was solved for the initially quiescent lattice, using a step size of $\Delta\tau = 0.05$, and produced the same numerical results as obtained for the analytic solution of Sec. 3.3. A similar result can also be obtained by simply making A_m very small (say, 0.001) in Eq. (4.9).

Second, in all our calculations we calculated the work done by the external force needed to move the first particle at a constant velocity of unity. This external force is, of course, just the negative of the force exerted on the first particle in the lattice by the second. A simple calculation reveals that in an infinitesimal time interval of $\Delta\tau$, the external force does an amount of work W, normalized by $1/2\ mu^2$, given by

$$W = \frac{1}{4A_m} \left\{ \exp\left[-2A_m(S_{2i} - S_{1i})\right] - \exp\left[-A_m(S_{2i} - S_{1i})\right] + \exp\left[-2A_m(S_{2f} - S_{1f})\right] - \exp\left[-A_m(S_{2f} - S_{1f})\right] \right\} \times (S_{1f} - S_{1i}) \qquad (4.15)$$

where i and f denote the values of S_1 and S_2 at the beginning and end of the time interval, respectively. The total work done on the system at time τ added to the initial kinetic energy of the first particle was then compared with the total internal energy of the lattice and the two results were found to agree.

Finally, we repeated a large number of our calculations varying the step size $\Delta\tau$ and consistently found that similar results were produced. It was found, however, that as A_m increased, it was necessary to decrease the step size, $\Delta\tau$, from values acceptable for the harmonic case.

5. PROPAGATION IN THE INITIALLY QUIESCENT, ANHARMONIC LATTICE

In this section, we shall be primarily concerned with the numerical solution of Eq. (4.9) for various values of the nonlinearity parameter, A_m. Prior to excitation by the shock, each of the atoms in the lattice is at rest in its equilibrium position. In the long-time limit, we observe well-defined, stable pulses (solitary waves) of constant amplitude propagating in the vicinity of the shock front. These solitary waves are rather unusual physical entities and we digress in Sec. 5.2 to discuss their characteristics and physical significance. In Sec. 5.3, we present an analytical approximation for the shape and amplitude of the solitary waves under certain limiting conditions and compare the results with our numerical solutions. Finally, we conclude this section by briefly considering the results of our calculations for shock propagation in a lattice whose atoms interact via the hard-sphere potential of Northcote and Potts[23] discussed in Sec. 2.

5.1 The Morse Interaction

We have solved Eq. (4.9) for various values of the nonlinearity parameter, A_m, which is a representation of both the strength of the compression and the anharmonicity of the lattice. [See Eq. (4.10).] The results of the calculation can be understood most easily by comparing the velocity-time trajectories for various particles in the lattice and indicating what conclusions can be drawn about the shock profile in general.

Velocity-time trajectories for several particles in the lattice are shown in Fig. 5 for the case in which the nonlinearity parameter, A_m, was equal to 0.2. In order to plot these trajectories on the same time scale, we have, in each case, readjusted the time axis so that at $\tau = 0$ the particle under consideration first feels the effect of the shock front. The actual time at which the front reaches the particle, denoted by τ_0, is indicated in the figure.

For a particle close to the driven end of the chain (particle 5 in the figure), the velocity variation is similar to that found for the harmonic lattice. (See Fig. 4, but note the change in scale.)

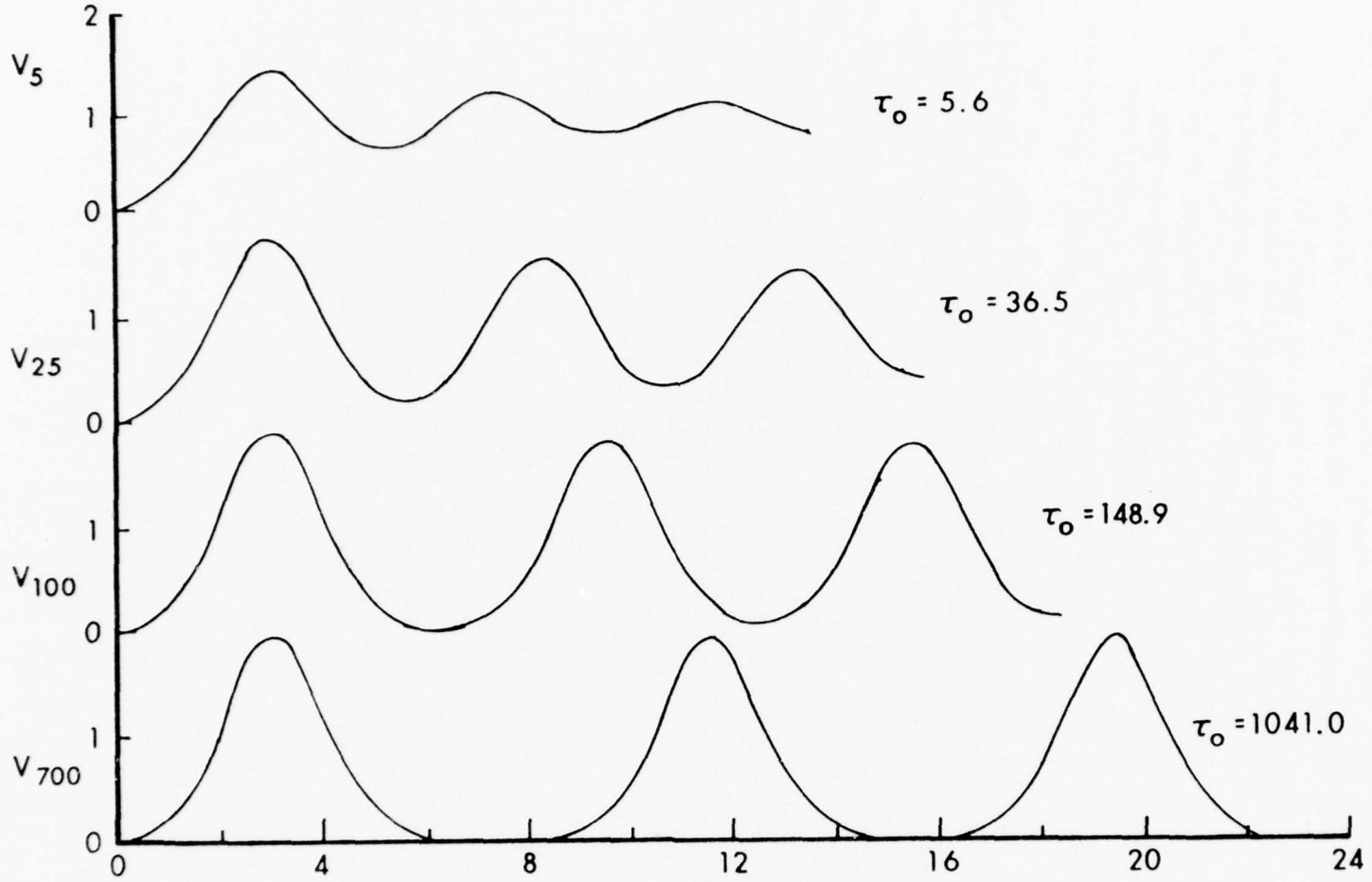

Figure 5. Velocity-time trajectories for the initially quiescent, Morse-potential lattice for the case $A_m = 0.2$.

Upon excitation by the shock wave, the particle velocity reaches an amplitude of about 1.44 and subsequently oscillates about unity, the compression velocity, with decreasing amplitude. By the time the shock front has reached the 25^{th} particle, the magnitude of the oscillations has increased. Meanwhile, the pulses have become narrower and more well defined. Physically, the early-time development of the oscillations is apparently governed by dispersion, but as the shock front propagates farther into the lattice, the nonlinear effects become increasingly important. These effects, of course, tend to steepen the pulse. It is interesting that the two effects become important in the reverse order from that observed by Zabusky and Kruskal[34] in their study of oscillations in a plasma.

By the time the front has reached the 100^{th} particle the shape of the pulses has become still more well defined and the amplitude appears to be approaching a constant maximum value of about 2. If we view a particular point in the lattice, the pulses in the vicinity of the shock front appear to propagate into the lattice from the compressed end. Since it is found that the velocity with which they propagate decreases with decreasing amplitude, they tend to spread apart as they propagate. When the shock front has reached the 700^{th} particle, we find that the leading pulses have evolved into a sequence of extremely well-defined excitations (solitary waves) and have indeed reached a constant amplitude of approximately 2. The pulses are more distantly spaced in time than when the front was at the 100^{th} particle, owing to the spreading effect discussed previously.

Therefore, for $A_m = 0.2$, the velocity trajectory for particles with $N \gtrsim 200$ can be described as follows: The trajectory initially varies along a sequence of solitary waves of essentially constant shape and amplitude, the number of these waves increasing slowly with increasing particle number. The velocity then undergoes damped oscillations about the value unity. Eventually these oscillations become negligible and the particle, for all practical purposes, then moves at a constant velocity equal to the compression velocity for all later times. This behavior is similar to that observed by Tasi[20] in his studies of a weakly nonlinear lattice described by a cubic interatomic potential.

Figure 6 shows a similar sequence of trajectories for the case in which the nonlinearity parameter, A_m, was equal to unity. Qualitatively,

34. N.J. Zabusky and M.D. Kruskal, "Interaction of Solitons in a Collisionless Plasma and the Recurrence of Initial States", Phys. Rev. Letters 15, 240 (1965).

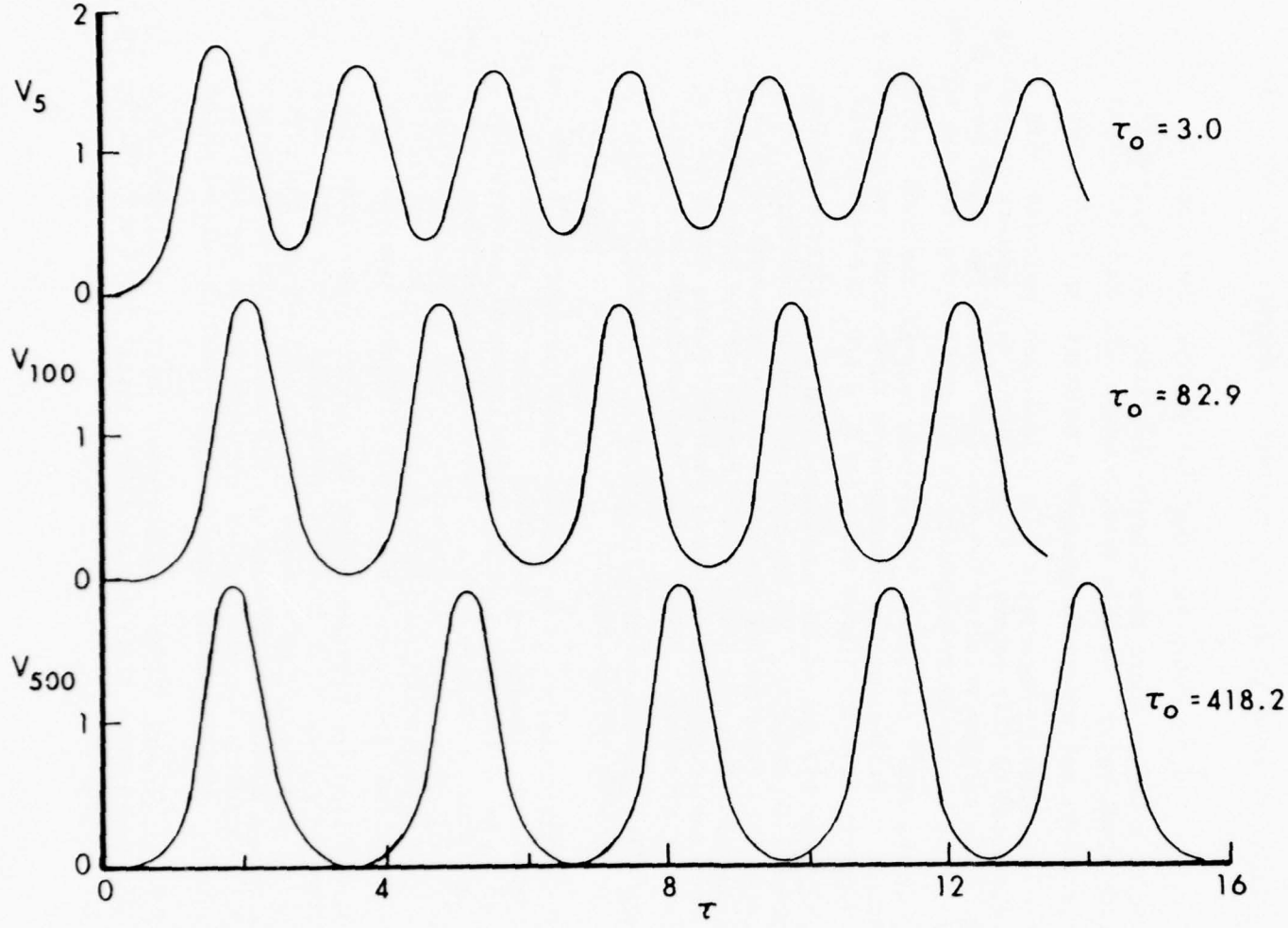

Figure 6. Velocity-time trajectories for the initially quiescent, Morse-potential lattice for the case $A_m = 1.0$.

the same description applies near the front except that the pulses are narrower, owing to the increased nonlinearity. A rather remarkable result of the calculations is that the solitary waves evolve to the same maximum amplitude for any nonzero value of A_m; the time necessary for the solitary waves to develop, however, increases with decreasing values of A_m.

For $A_m = 1.0$, we again find that the solitary-wave train is followed by a region where the velocity oscillates with decreasing amplitude about unity. In this case, however, the oscillations do not decay entirely, but appear to approach a constant amplitude. This behavior was noted by Strenzwilk[35] in calculations performed with the model discussed in this report. We illustrate this feature by plotting in Fig. 7 the maximum velocity for particles behind the front for both values of the nonlinearity parameter at a time when the front is approximately at the 480^{th} particle. The minimum velocity for each case can be obtained by reflecting the corresponding curve about the value unity. It is apparent from the figure that, for $A_m = 1.0$, the velocity of particles near the end of the compressed region oscillates between the values 1.54 and 0.46. We observed no tendency for these oscillations to decay during the course of the computation. This result suggests that the oscillations far behind the front approach a constant amplitude which decreases with decreasing values of the nonlinearity parameter. For $A_m = 0.2$, this amplitude is so small that the particles are essentially moving at a constant velocity equal to the compression velocity.

The question arises as to whether these oscillations might lead to a temperature rise behind the front. During the calculation, there appeared to be no tendency towards randomization of the velocity; in fact, the velocity of each particle continued to vary along well-defined oscillations. The absence of thermalization is illustrated in Fig. 8 which shows the velocity distribution function, f, for the first 250 particles in the lattice at two slightly different times for $A_m = 1.0$. The distribution function represents the number of particles with velocities in a particular interval, normalized to the total number of particles. For the system to be in thermal equilibrium, the distribution should be constant in time and the profile should correspond to a Maxwellian distribution about unity corresponding to the equilibrium temperature. It is apparent from the figure that the distribution

35. D.F. Strenzwilk, "Effect of Different Initial Accelerations on the Subsequent Shock Profile in One-Dimensional Lattices", BRL Report (to be published).

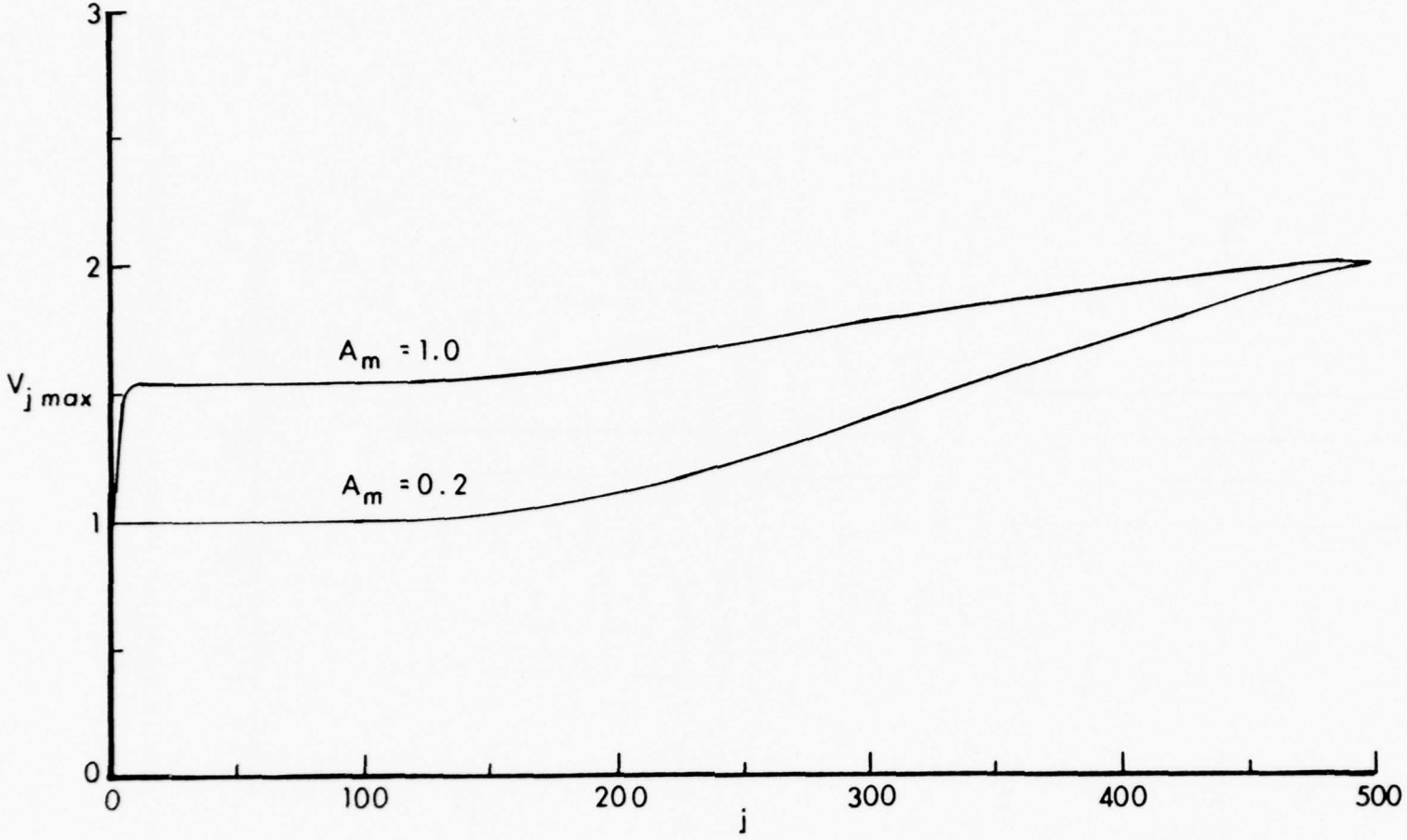

Figure 7. Maximum particle velocity behind the front for the cases $A_m = 0.2$ and $A_m = 1.0$.

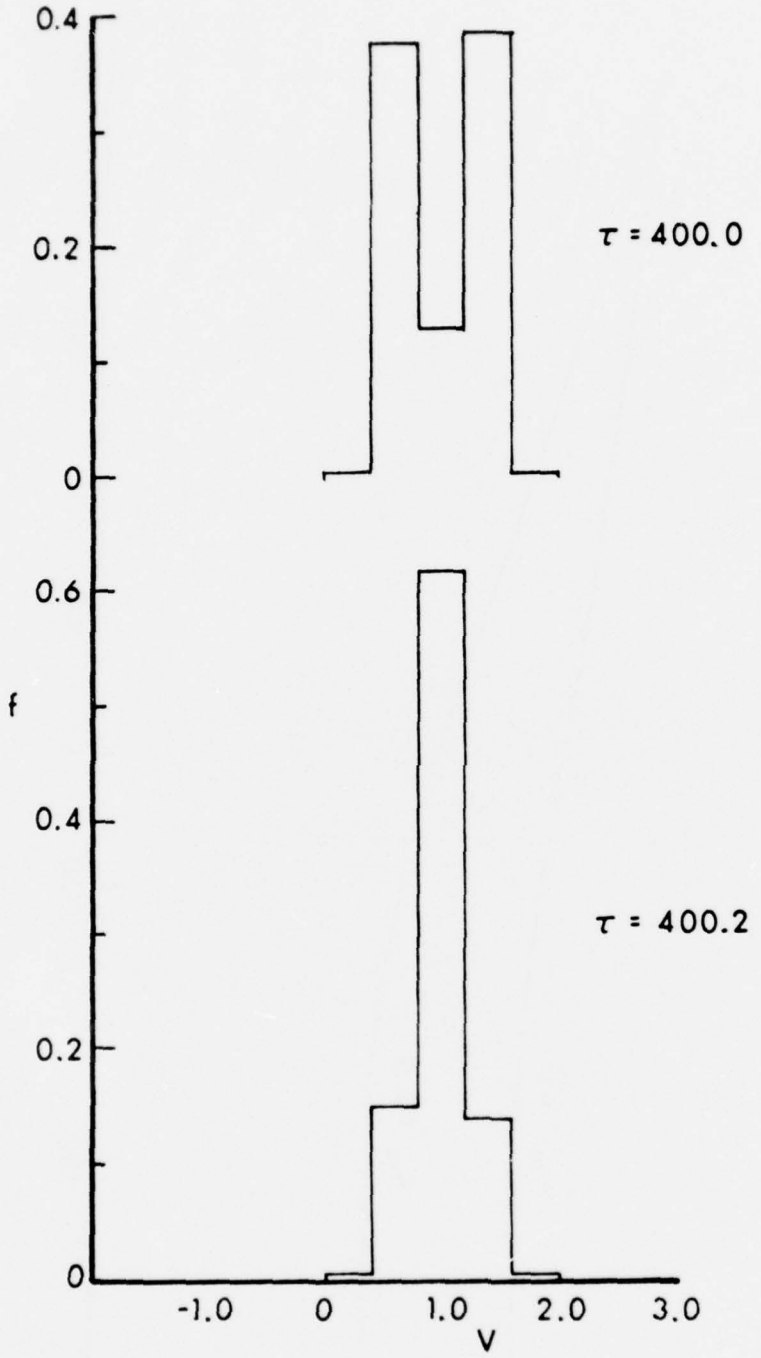

Figure 8. Velocity distribution function for the initially quiescent, Morse-potential lattice at two times.

function for this case is not Maxwellian. In fact, the shape of the distribution curve changes dramatically with time, depending on where in the oscillation cycle most particles happen to be when the distribution is sampled. We conclude, therefore, that shock compression in the initially quiescent lattice does not lead to a temperature rise behind the front.

The conclusions which can be drawn from our calculations as well as preceding studies[16-21] of shock propagation in an anharmonic, quiescent, one-dimensional lattice can be summarized as follows: (1) The shock speed is, on the average, constant and increases with increasing A_m. The calculation is quite simple from the computer data and will not be carried out here. (2) The early development of the shock profile is governed by dispersion which leads to an oscillatory velocity profile. As these oscillations grow in amplitude, resulting in larger relative displacements, nonlinear effects become important. Eventually a point is reached at which the nonlinear effects, which tend to steepen the pulse, exactly balance the dispersion, which tends to broaden it. Solitary waves propagate in the vicinity of the front at this time. (3) The effects of nonlinearity become more pronounced with increasing A_m for a given distance into the lattice, and with increasing distance into the lattice for a given A_m. These effects are made evident in two ways. The solitary waves develop more quickly in more nonlinear lattices, and, for a given A_m, the number of solitary waves increases as the shock propagates farther into the lattice. (4) The energy deposited into the lattice by the shock front appears either as potential energy due to compression of the lattice or as ordered translational energy of the particles behind the front. There is no thermalization of the energy so that the compressed lattice remains at zero temperature after the shock has passed. (5) The shock profile is not steady in time because of the spreading effect of pulses of different amplitude discussed previously. The last two results are in obvious contradiction to the usual assumptions in continuum treatments of shock propagation.

5.2 Characteristics and Physical Significance of Solitary Waves

Solitary waves, such as the ones discussed in the last subsection, have been observed to propagate in other nonlinear, dispersive media. They represent particular solutions to nonlinear, differential equations which describe wave propagation in certain continuous media and in the so-called "Toda" discrete lattice[36,37]. Two excellent review

36. M. Toda, "Vibration of a Chain With Nonlinear Interaction", J. Phys. Soc. Japan 22, 431 (1967).
37. M. Toda, "Wave Propagation in Anharmonic Lattices", J. Phys. Soc. Japan 23, 501 (1967).

articles[38,39] have recently been written which discuss the properties of solitary waves and the sort of systems to which they apply. The article by Toda emphasizes in particular propagation in the nonlinear lattice.

Until recently, solitary waves were considered to be only of academic interest. Since they represented only particular solutions to differential equations, it was suspected that they would exist only under a rather special set of initial conditions. Consequently, it was felt that their significance to an arbitrary initial-value problem was minimal. At any rate, it was believed that, upon collision, two solitary waves would scatter irreversibly, so that their presence would, at most, be a transient effect.

The last assumption was disproved by Zabusky and Kruskal[34] in their numerical solution of the Korteweg-de Vries equation describing plasma waves. Solitary waves of various velocities were allowed to collide and, after collision, were observed to maintain their original shapes. The term "solitons" was coined by Zabusky and Kruskal to refer to solitary waves which remained stable upon collision with one another. The most significant, and rather startling, conclusion from these investigations is that, for a system in which solitons propagate, one can expect "randomization" of the energy or thermal equilibrium to occur only after extremely long times, if ever.

Zabusky and Kruskal suggested that the existence of solitons could explain the paradoxical results obtained in the famous Fermi, Pasta, Ulam computer study[7] in the 1950's. These investigators had excited a single normal mode in a weakly anharmonic lattice and had observed that, rather than becoming equipartitioned among the various normal modes, the energy flowed periodically among only certain of the modes. In addition, after some recurrence time, the system returned to its initial state, apparently disproving the ergodic hypothesis[40] of statistical mechanics. Various explanations[41-43] of the results have been offered,

38. A.C. Scott, F.Y.F. Chu and D.W. McLaughlin, "The Soliton: A New Concept in Applied Science", Proc. IEEE 61, 1443 (1973).
39. M. Toda, "Studies in a Nonlinear Lattice", Physics Reports 18C, 1 (1975).
40. R.C. Tolman, The Principles of Statistical Mechanics (Oxford University Press, New York, 1938), Chap. 3.
41. J. Ford, "Equipartition of Energy for Nonlinear Systems", J. Math. Phys. 2, 387 (1961).
42. J. Ford and J. Waters, "Computer Studies of Energy Sharing and Ergodicity for Nonlinear Oscillator Systems", J. Math. Phys. 4, 1293 (1963).
43. E.A. Jackson, "Nonlinear Coupled Oscillators. I. Perturbation Theory; Ergodic Problem", J. Math. Phys. 4, 551 (1963).

but the suggestion of Zabusky and Kruskal seems to be the most conclusive. Since their study, there has been renewed interest in the study of solitary-wave behavior, as can be witnessed from the review articles cited previously.

5.3 Analytic Approximation for Solitary Waves in the Continuum Limit

A comparison of the solitary-wave profile for $A_m = 0.2$ (Fig. 5) with that for $A_m = 1.0$ (Fig. 6) indicates that the solitary wave becomes broader as the nonlinearity parameter decreases. This trend suggests that for sufficiently small values of A_m it might be possible to derive an analytic approximation to the solitary-wave profile from the continuum limit of the equations of motion. Therefore, we now consider the case in which the nonlinearity parameter is small and take the continuum limit of Eq. (4.9). For small values of A_m, the exponential terms in Eq. (4.9) can be expanded, and if we retain only the lowest-order nonvanishing terms in A_m, we obtain

$$\ddot{S}_k = \frac{(S_{k+1} + S_{k-1} - 2S_k)}{4} \left[1 - \frac{3}{2} A_m (S_{k+1} - S_{k-1}) \right] . \tag{5.1}$$

The right-hand side of Eq. (5.1) is just the force derived from the cubic interatomic potential used by Tasi[19-21] and by Manvi et al.[16-20].

We now assume that $S_{k\pm1}$ can be related to S_k by a Taylor expansion about the lattice constant, a_0, equal to zero, i.e., a continuum approximation. Letting $S_k = S$, we have

$$S_{k\pm1} = S \pm \frac{\partial S}{\partial k} + \frac{1}{2} \frac{\partial^2 S}{\partial k^2} \pm \frac{1}{3!} \frac{\partial^3 S}{\partial k^3} + \frac{1}{4!} \frac{\partial^4 S}{\partial k^4} + \cdots \tag{5.2}$$

Substituting Eq. (5.2) into Eq. (5.1) and retaining terms through the fourth derivative produce the result

$$\frac{\partial^2 S}{\partial \tau^2} = \frac{1}{4} \frac{\partial^2 S}{\partial k^2} + \frac{1}{48} \frac{\partial^4 S}{\partial k^4} - \frac{3A_m}{4} \frac{\partial^2 S}{\partial k^2} \frac{\partial S}{\partial k} . \tag{5.3}$$

Equation (5.3) is the so-called Zabusky equation[39]. If we neglect the last two terms, we get the ordinary linear wave equation. (Recall that the sound speed in the harmonic lattice was one-half in our nondimensional units.) The last term on the right-hand side represents the lowest-order nonvanishing term in the nonlinearity, whereas the fourth-derivative term must be kept to account for dispersion.

Equation (5.3) is obviously difficult to solve in general, but since we are only interested in determining what well-defined pulses the lattice can support, we assume a traveling-wave solution of the form

$$S = S(k - C\tau) = S(y) \tag{5.4}$$

where C is the solitary-wave propagation velocity. Substitution of Eq. (5.4) into Eq. (5.3) and noting that

$$V = \frac{\partial S}{\partial \tau} = - C \frac{dS}{dy} \tag{5.5}$$

$$\frac{\partial S}{\partial k} = \frac{dS}{dy} \quad , \tag{5.6}$$

yield

$$12C(4C^2 - 1)V' = CV''' + 36\, A_m VV' \tag{5.7}$$

where the primes denote differentiation with respect to y. Equation (5.7) can be integrated once and, applying the boundary conditions that V and its derivatives vanish at $\pm \infty$, we obtain

$$12C(4C^2 - 1)V = CV'' + 18\, A_m V^2 \quad . \tag{5.8}$$

Multiplying Eq. (5.8) by the integrating factor, V′, and integrating once more yield

$$12C(4C^2 - 1)V^2 = C(V')^2 + 12\, A_m V^3 \quad , \tag{5.9}$$

whence

$$V' = \left[12(4C^2 - 1)V^2 - 12\, A_m V^3/C \right]^{1/2} \quad . \tag{5.10}$$

Equation (5.10) can be solved for y to produce

$$y = \int \frac{dV}{\left[12(4C^2 - 1)V^2 - 12\, A_m V^3/C \right]^{1/2}} \quad . \tag{5.11}$$

The integration in Eq. (5.11) is elementary and produces the result

$$V = \frac{(4C^2 - 1)C}{A_m} \operatorname{sech}^2 \left[\sqrt{3(4C^2 - 1)}\; y \right] . \tag{5.12}$$

Equation (5.12) should represent an approximation to the amplitude and shape of the solitary waves for sufficiently small values of A_m provided the continuum approximation is valid. To check the results, we obtained from our computer data values of the propagation velocity C for different values of A_m, substituted them into Eq. (5.12), and compared the results with the results of our numerical calculations. The results are indicated in Table II in which we show the value of A_m; the propagation velocity, C; the soliton amplitude, Å; and the full width of the soliton at half maximum, Δ. The last two columns show the corresponding values as calculated from Eq. (5.12) using values for C contained in column 2. The results are in fair agreement (within about 15%) for the smallest value of A_m, but the difference between computed and analytical results increases rapidly with increasing A_m. Figure 9 shows a comparison of the numerical and analytical wave profiles for $A_m = 0.1$.

TABLE II. ANALYTICAL AND COMPUTATIONAL VALUES OF SOLITARY-WAVE AMPLITUDES AND WIDTHS. VELOCITIES ARE EXPRESSED IN NUMBER OF PARTICLES PER UNIT OF NONDIMENSIONAL TIME.

		Computational		Analytical	
A_m	C	A	Δ	A	Δ
0.1	0.59	2.0	3.1	2.3	2.8
0.2	0.68	2.0	2.3	2.9	1.6
1.0	1.19	2.0	1.0	5.6	0.20

5.4 The Hard-Sphere Model of Northcote and Potts

Northcote and Potts[23] have suggested a potential in which the atoms are assumed to have a finite diameter, d, and interact with one another via harmonic forces. Between collisions, the motion is equivalent to that of a harmonic lattice, but, upon collision, the atoms exchange momenta. This extremely nonlinear potential was used by Northcote and Potts to repeat the Fermi, Pasta, Ulam problem in an effort to determine whether the strong nonlinearity would cause the system to approach thermal equilibrium. Their results suggested that the system did equilibrate after excitation of a single mode. That thermalization of

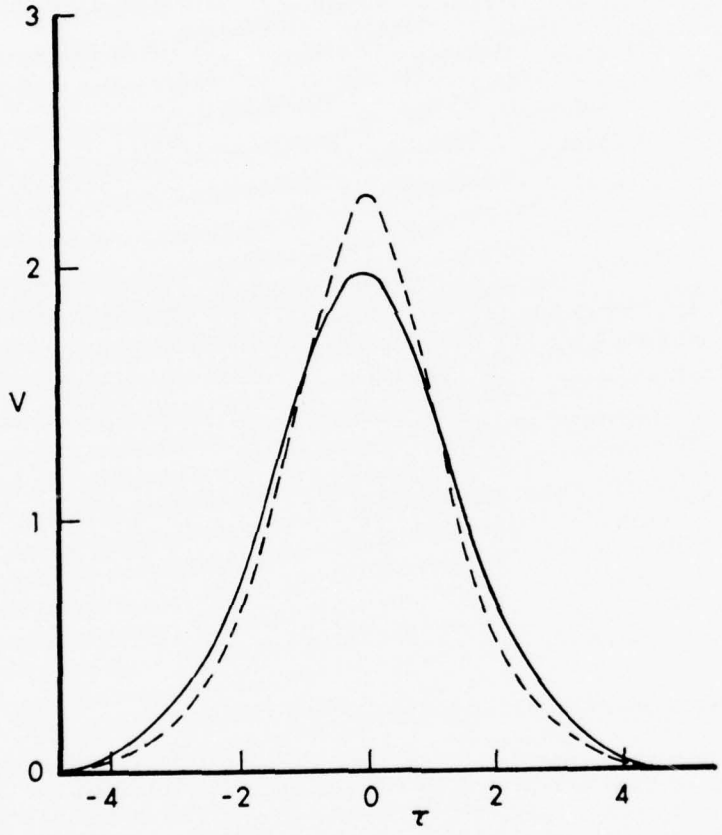

Figure 9. Comparison of numerical and analytical solitary-wave profiles for $A_m = 0.1$. The solid and dashed lines represent the numerical and analytic solutions, respectively.

of the energy occurred (perhaps) led Montroll[44] to speculate that this potential did not possess solitary-wave solutions.

We have modified our computer code to treat a hard-sphere lattice subjected to shock compression. Our interest was to determine both whether equilibration of the energy occurred behind the front and whether the energy could be propagated in the form of solitary waves. For purposes of calculation, we assumed a nondimensional diameter (real diameter normalized by u/ω_0) of 0.75 and a nondimensional lattice spacing,

$$R = \frac{a_0\omega_0}{u} \quad , \tag{5.13}$$

of 3.0. Again, we assumed that the atoms of the lattice were at rest prior to excitation by the shock.

Figure 10 shows the velocity-time trajectories of the 25^{th} and 50^{th} particles in the lattice subsequent to excitation by the shock. In the vicinity of the front, we find again a series of well-defined pulses having constant amplitude and width. The amplitude is approximately 1.6. It should be observed that well-developed solitary waves are propagating in the vicinity of the front as early as the 25^{th} particle. The increased nonlinearity causes the solitary waves to form more rapidly than in the Morse-potential cases we studied.

From Fig. 10, it may be noted that, at any given particle, there appears to be a tendency for the solitary waves to become more distantly spaced in time with increasing time. It is interesting that this is the opposite effect from that observed in the case of the Morse potential. The spreading can be seen more easily in Fig. 11 in which is plotted the velocity as a function of particle number at three different times. The figure indicates that the length of "dead spaces" or regions of the lattice in which the particle velocity is essentially zero increases with both distance from the front and with time. In addition, there appears to be no gradual decay of the pulse amplitude as we approach the region of uniform motion behind the front, but rather there is a sudden transition between this region and the region of solitary-wave propagation.

The reasons for the differences in detail between the hard-sphere case and the Morse-potential case are presently not clear to us. It is nevertheless interesting that both predict a nonsteady profile and no temperature rise behind the front as can be observed from Fig. 11. In addition, the hard-sphere potential does appear to be able to support the propagation of solitary waves at least under this rather ordered set of initial conditions.

---

44. E. Montroll, in "Proceedings of the Explosives Chemical Reactions Seminar", ARO-D Report 70-4, Durham, NC, 1968, p. 145.

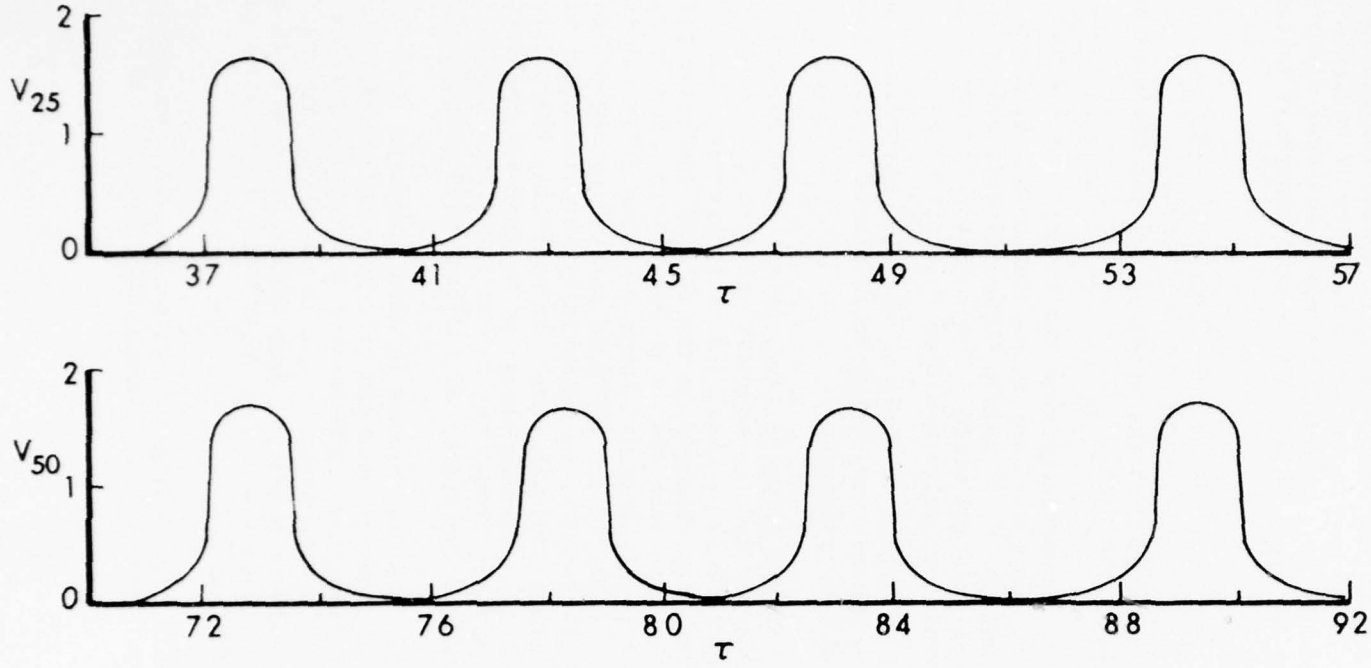

Figure 10. Velocity-time trajectories for two particles in the hard-sphere lattice.

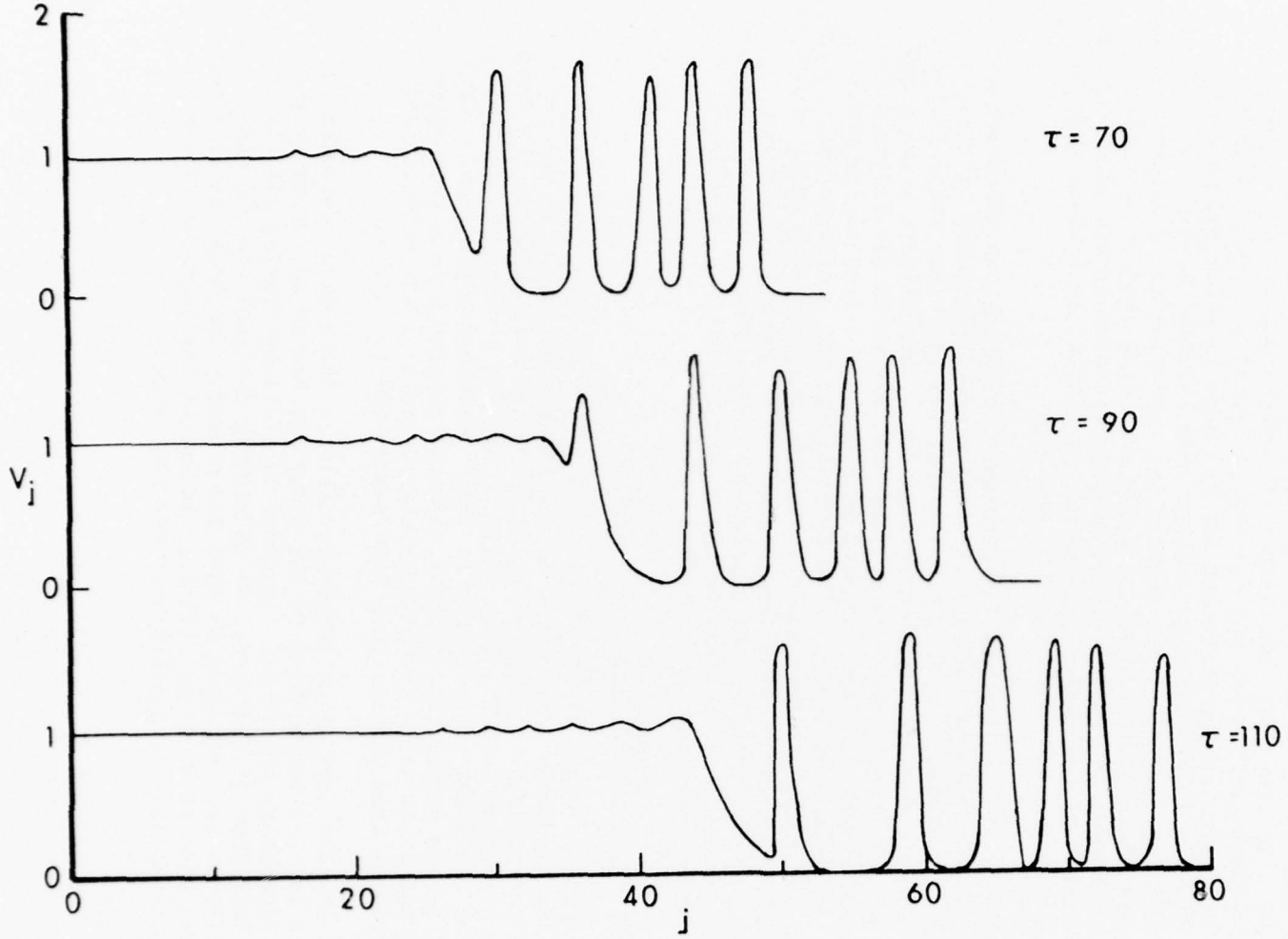

Figure 11. Velocity as a function of particle number in the hard-sphere lattice for three times.

6. PROPAGATION IN THE ANHARMONIC LATTICE AT NONZERO INITIAL TEMPERATURE

The calculations of the preceding section represent somewhat of a compromise to physical reality because, as we have emphasized, it was assumed that the particles were initially at rest in their equilibrium positions. Consequently, the effect of nonzero ambient temperature upon the shock profile has not yet been examined. In this section, we discuss calculations performed for the case in which the particles in the lattice were allowed to undergo some initial thermal oscillations prior to being excited by the shock. Our intention is to determine which, if any, of the anomalous results of the preceding section (nonsteady profile, absence of equilibration, propagation of solitary waves) are a manifestation of the rather ordered set of initial conditions used in that calculation.

In Sec. 6.1, we discuss the procedure for doing the calculations and in Sec. 6.2 the method for preparing a one-dimensional lattice in thermal equilibrium. In Sec. 6.3, various velocity-time trajectories are discussed as before and we observe high-amplitude solitary waves propagating amid a thermal background. The solitary waves are isolated from the thermal background and compared with those obtained in the previous section. In Sec. 6.4, we observe a "collision" or nonlinear interaction between two solitary waves and discuss the consequence of their stability. In Sec. 6.5, we investigate the possibility of thermal equilibrium behind the shock front and calculate the thermodynamic variables of interest. Finally, in Sec. 6.6, we examine the extent to which the steady-state conservation equations are satisfied.

6.1 Method for Performing Calculations

Since the shock front travels at a finite speed into the lattice and since our major interest is in the shock profile, it is clearly unnecessary to monitor the particles which lie well ahead of the front. In the preceding section, this posed no problem because the particles ahead of the front were at rest in their equilibrium positions. Consequently, we simply provided our computer program with a test which caused the calculation to include only particles whose velocity and displacement were greater than some small number.

A similar test is no longer possible in the present calculation because the particles ahead of the front are now in motion prior to being excited by the front. In order to avoid monitoring all the particles ahead of the front, it is clearly desirable to add the particles in segments only as they are needed. One might still expect, however, that it would be difficult to detect the location of the shock front in the lattice particularly for weak shocks.

An extremely clever solution to the problem was suggested to us by Tsai[45]. We simulate the semi-infinite lattice at $\tau = 0$ by a series of identical segments, each containing n particles in thermal equilibrium, as shown in Fig. 12. In other words, the velocities and displacements of the particles in the chain are initially related by the periodic conditions

$$V_m(0) = V_{jn+m}(0)$$

$$S_m(0) = S_{jn+m}(0) \quad , \quad j = 1,2,\ldots \ , \quad m = 1,2,\ldots n \quad .$$

The first particle is then subjected to steady compression at a nondimensional velocity of unity as before and, as a result, a shock wave proceeds through the chain.

Consider the j^{th} particle assumed to be located in the first segment. Before the shock front reaches this particle, its motion is identical to the $j+n^{th}$ particle because these atoms are acted upon by identical forces and had identical initial conditions. Working our way backwards from the j^{th} particle, we locate the first particle whose displacement and velocity differ appreciably from those of the symmetric particle in the second segment and, thereby, determine exactly the location of the front at any time τ. Furthermore, until the shock reaches the n^{th} particle, it is necessary to solve the equations of motion for only the first two segments since the particles in all the remaining segments will have trajectories identical to the corresponding particles in the second segment. (In order to calculate the force from the right on the $2n^{th}$ particle, the displacement of the $2n+1^{st}$ particle is required. However, we do not have to monitor this particle since its displacement is equivalent to that of the $n+1^{st}$ particle.) When the shock front nears the n^{th} particle, the particles in the third segment are included in the computation. The shock front is located in the same manner as before, and the process repeated as often as necessary to complete the calculation. It is therefore necessary to monitor at most 2n particles ahead of the shock front at any time, the last n representing the equilibrium conditions of the chain ahead of the shock. For purposes of calculation, n was taken to be 100.

6.2 Preparation of Initial Segment in Thermal Equilibrium

We begin this subsection by considering the properties of a one-dimensional chain of atoms in thermal equilibrium. We then discuss how we may artificially prepare the lattice so these properties are satisfied.

45. D.H. Tsai, private communication.

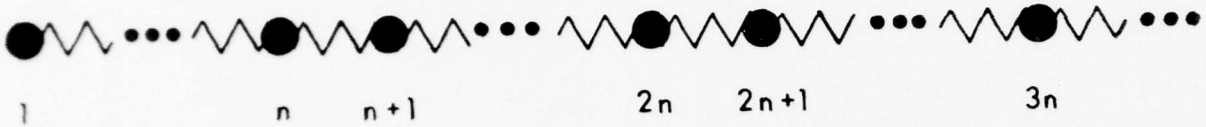

Figure 12. Construction of a semi-infinite chain from a sequence of initially identical segments.

Consider a chain of n particles obeying cyclic boundary conditions such that the first and n^{th} atoms are connected. The chain is assumed to be in thermal equilibrium at temperature T. From the definition of equilibrium, the probability that the system occupies a particular differential volume in phase space is given by the distribution function

$$F(v_1,\ldots v_n,\ x_1,\ldots\ x_n)dv_1\ldots dv_n dx_1\ldots dx_n = \frac{1}{Z}\exp\left[-\left(\sum_i \frac{mv^2_i}{2} + \Phi\right)/kT\right]$$

$$dv_1\ldots dv_n dx_1\ldots dx_n \qquad (6.1)$$

where Z is the partition function which normalizes the distribution to unity and Φ is the total potential energy of the lattice. The probability that particle j has velocity between v_j and v_j+dv_j regardless of its displacement and regardless of the velocities and displacements of the remaining particles of the lattice is obtained by integrating Eq. (6.1) over all displacements and all velocities except the j^{th}. If we assume a velocity-independent potential, the result is

$$F(v_j)dv_j = \frac{1}{z}\exp\left[-mv^2_j/(2kT)\right]\quad dv_j \qquad (6.2)$$

where

$$z = \int_{-\infty}^{\infty} \exp\left[-mv^2_j/(2kT)\right]\ dv_j \quad . \qquad (6.3)$$

Equation (6.2) indicates that the velocities of all particles are distributed according to a Maxwellian distribution at temperature T, regardless of the form of the potential interaction as long as it is velocity independent. Consequently, the mean (ensemble average) square velocity of any particular particle is given by

$$\langle v^2\rangle = \frac{1}{z}\int_{-\infty}^{\infty} v^2 \exp\left[-mv^2/(2kT)\right]dv = kT/m\ , \qquad (6.4)$$

and the mean thermal velocity by

$$v_T = \sqrt{\langle v^2\rangle} = \sqrt{kT/m} \quad . \qquad (6.5)$$

If the lattice discussed above were harmonic, it is well known that the total energy contained in the lattice is given by

$$\varepsilon = nkT \quad . \tag{6.6}$$

On the average, half of the energy is potential and half kinetic. If an initial energy given by Eq. (6.6) is put into an anharmonic lattice and the lattice allowed to come to thermal equilibrium, it will equilibrate at some slightly different temperature T' owing to the difference in the harmonic and anharmonic potentials. If the lattice is only slightly anharmonic, however, the temperature T' should not be appreciably different from T and Eq. (6.6) will be a reasonable estimate of how much energy to initially put into the lattice to correspond to an anharmonic lattice in equilibrium at temperature T. Before proceeding further, it is convenient to nondimensionalize the quantities of interest as before. The thermal velocity, normalized by the compression velocity, then is

$$V_T = \frac{v_T}{u} = \left(\frac{kT}{mu^2}\right)^{\frac{1}{2}} \quad , \tag{6.7}$$

and, the total energy in the lattice, normalized by the kinetic energy of the first particle, is

$$E = \frac{\varepsilon}{\frac{1}{2}mu^2} = \frac{2nkT}{mu^2} = 2n\ V_T^{\,2} \quad . \tag{6.8}$$

The thermal velocity, V_T, is the only additional parameter that must be specified in the computer input.

In order to prepare our initial segment of n particles in thermal equilibrium, we generated a set of n-1 random velocities obtained from a Maxwellian velocity distribution. The velocity of the n^{th} particle was determined from the condition

$$\sum_{j=1}^{n} V_j = 0 \quad , \tag{6.9}$$

imposed so as to impart no net momentum to the chain. Each particle in the chain was assumed to be in its equilibrium position initially (no potential energy) and the velocities were scaled by a constant factor c. This factor was chosen so that the initial nondimensional energy in the chain was given by Eq. (6.8). Thus, we required

$$c^2 \sum_{j=1}^{n} V_j^{\,2} = 2n\ V_T^{\,2} \tag{6.10}$$

which determines the factor c.

Having obtained the scaled velocities in the manner discussed above, we assigned them to each of the n particles in the segment. The lattice was then allowed to oscillate freely and we employed a number of checks to insure that it was actually in a state of thermal equilibrium. First, we calculated the velocity distribution function at several times and found that the function was constant in time and essentially Maxwellian. Second, we calculated the time average of the velocity squared for several of the atoms in the lattice, obtained by evaluating the expression

$$\overline{V_j^2} = \frac{1}{\Delta\tau} \int_{\tau_1}^{\tau_2} V_j^2 (\tau) d\tau \qquad (6.11)$$

where $\Delta\tau$ is a time long compared with unity. We found that the time average agreed with the average taken over all particles in the system at any time, viz.,

$$< V^2 > = \frac{1}{n} \sum_j V_j^2 (\tau) \quad . \qquad (6.12)$$

Third, we found that the total kinetic and potential energies in the lattice remained essentially constant in time. As we pointed out before, one would expect, for a harmonic lattice, that the kinetic and potential energies would be equal and each given by $n v_T^2$. For the anharmonic case, this is no longer true and we found generally that the kinetic energy was slightly larger than the potential. Finally, we calculated the local potential and kinetic energies by averaging over a few (say, 25) particles within the segment and found that these were roughly constant in both space and time. Some deviations did occur, but these were attributed to the fact that relatively few particles were contained in the average.

We should point out that we have studied equilibration of the chain when the ends were subjected to various boundary conditions, but have found that only the cyclic condition produced reasonable results. For the case of fixed end conditions, we found that the unequal forces exerted (at any given time) upon the ends of the chain by the fixed particles tended to cause the center of mass of the chain to drift first in one direction and then in the other. This resulted in rather large-scale displacements of the interior particles from their equilibrium positions. For the case of free ends, we found extremely large displacements of the particles particularly toward the ends of the chain. It is commonly accepted that, for sufficiently large systems, the end conditions do not affect the bulk properties of the system. Apparently, however, a chain of 100 particles is not large enough to neglect such effects. The general desirability of using periodic boundary conditions in computer studies of small systems has been

discussed elsewhere[46].

We have considered in our calculations various values of the thermal velocity V_T. If we choose as reasonable values

$$T = 300°k$$

$$m = 10^{-25} kg$$

$$u = 500 \text{ m/s},$$

we obtain

$$V_T = \left(\frac{kT}{mu^2} \right)^{\frac{1}{2}} \sim 0.4 \quad . \tag{6.13}$$

Consequently, at room temperature we do not expect the thermal velocity to be negligible with respect to the compression velocity. Furthermore, as T decreases, V_T only decreases as $\sqrt{T}$, and it is likely that only at very low temperatures indeed can one expect that neglecting the thermal velocity is a realistic assumption. It was this consideration which prompted the calculations of this section.

6.3 Velocity-Time Trajectories and Propagation of Solitary Waves

In this subsection, we discuss the velocity-time trajectories obtained when the equilibrated lattice discussed above was subjected to shock compression for the case in which $A_m = 1.0$ and $V_T = 0.5$. Figure 13 shows the trajectories for three particles in the lattice, namely, 100, 200, and 300. Again, the time scales have been adjusted so that, at time $\tau = 0$, the particle first feels the effect of the shock. Referring to the 100^{th} particle and to the pulses labelled A,B, and C in the graph, we observe some evidence of high-amplitude solitary waves propagating amid a thermal background. Because of the background, however, the shapes of the pulses are not so well defined as in the case for which the particles were initially at rest in their equilibrium positions. Recalling that propagation is occurring toward the left, we see that by the time the front has reached the 200^{th} particle, pulse C has begun to approach pulse B, whereas pulse A has moved considerably farther ahead of B. At particle 300, pulse A has moved still farther ahead of B, but it appears that pulses B and C are nearly the same distance apart as when the shock was at the 200^{th} particle.

46. B.J. Alder and T.E. Wainwright, "Studies in Molecular Dynamics. I. General Method", J. Chem. Phys. 31, 459 (1959).

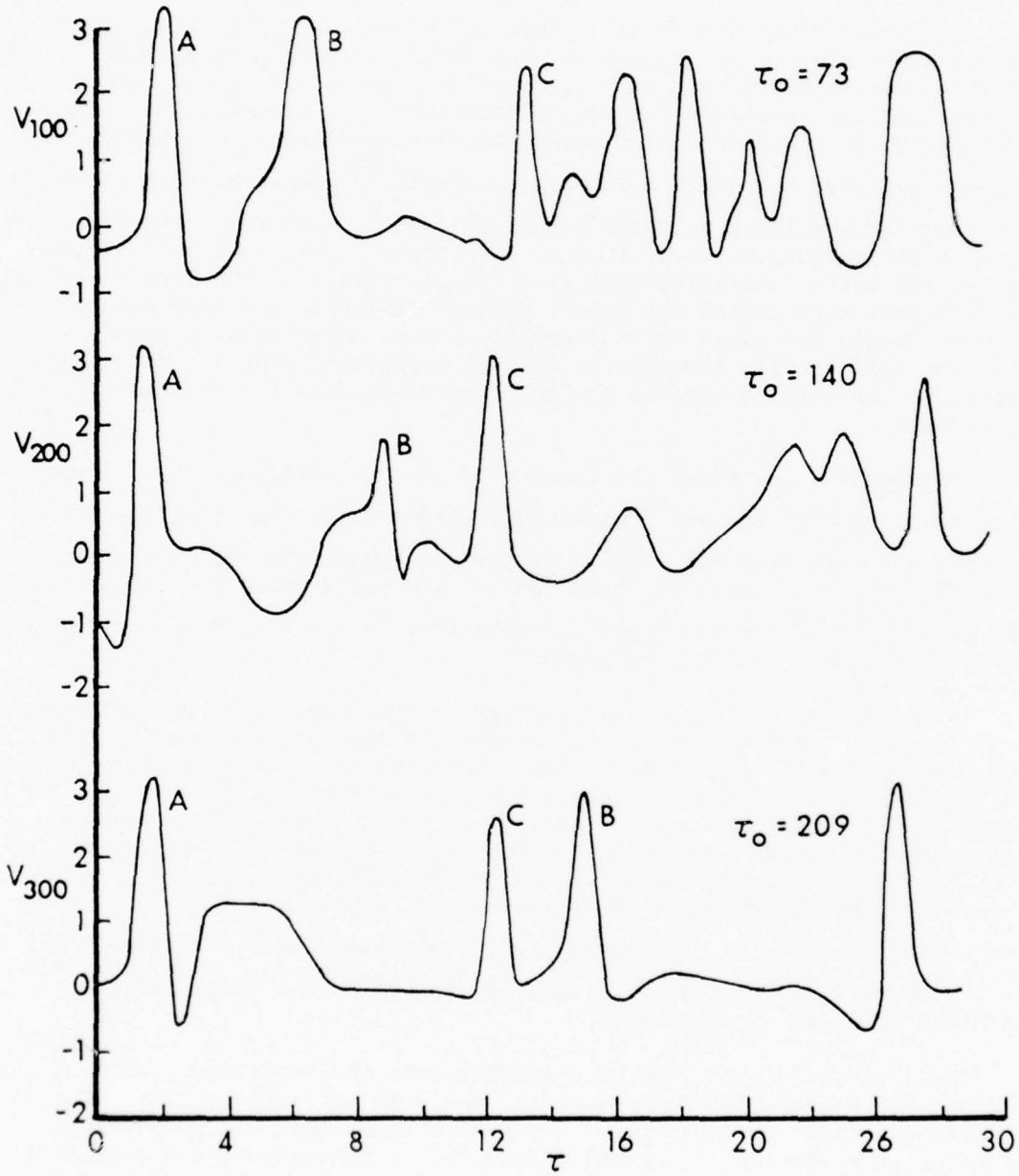

Figure 13. Velocity-time trajectories for three particles in a Morse-potential lattice with nonzero initial temperature. The particle first feels the effect of the shock at the time τ_o.

We are therefore led to speculate that B and C crossed while propagating between the 200^{th} and 300^{th} particles.

The above observations are rather imprecise. In fact, it is not really clear whether the pulses we have observed are high-amplitude solitary waves interacting with a thermal background or simply rather extreme, perhaps unstable thermal oscillations. In an effort to resolve this point, we redid the calculation, but instantaneously stopped the compression when the shock front was at the 140^{th} particle. The remaining particles of the lattice, those beyond the 140^{th}, were then placed at rest in their equilibrium positions. Essentially, we had a hot, shock-compressed lattice directly next to a cold lattice. If the large-velocity oscillations were indeed the result of high-amplitude solitary waves, then we should see these waves propagating with superacoustic speeds into the cold lattice leaving the thermal background behind. We should, therefore, be able to isolate the solitary waves from the thermal background.

Figure 14 illustrates the results of the calculation. The velocity-time trajectory of the 145^{th} particle is plotted for the case in which the shock compression was stopped at the 140^{th} particle and the remaining particles placed at rest in their equilibrium positions. For comparison, the trajectory of the 145^{th} particle obtained in the original calculation is shown in lower part of the graph.

From Fig. 14 we indeed find solitary waves propagating out into the cold lattice. Unlike for the case studied in the last section, however, the pulses apparently do not evolve to the same constant amplitude and, at the head of the front, the amplitudes are higher than for the case of the initially cold lattice. Comparison of the location of the peaks of the pulses in the upper and lower parts of the figure again emphasizes that the original pulses which we saw are solitary waves propagating upon a thermal background. Consequently, the labels A,B, and C, correspond to the same pulses observed propagating between the 100^{th} and 300^{th}particles in Fig. 13; the label, D, refers to the fourth solitary wave not discussed previously.

We have calculated from our computer data the amplitudes, and propagation velocities of waves A,B,C, and D in the cold lattice. The results are shown in Table III. We observe again that the propagation velocity increases with increasing amplitude. Consequently, a spreading effect will be introduced as before which will prevent the profile from approaching a steady state. We can also anticipate from the table that pulses B and C will eventually "collide". A simple calculation reveals that the collision should take place in the vicinity of the 280^{th} particle

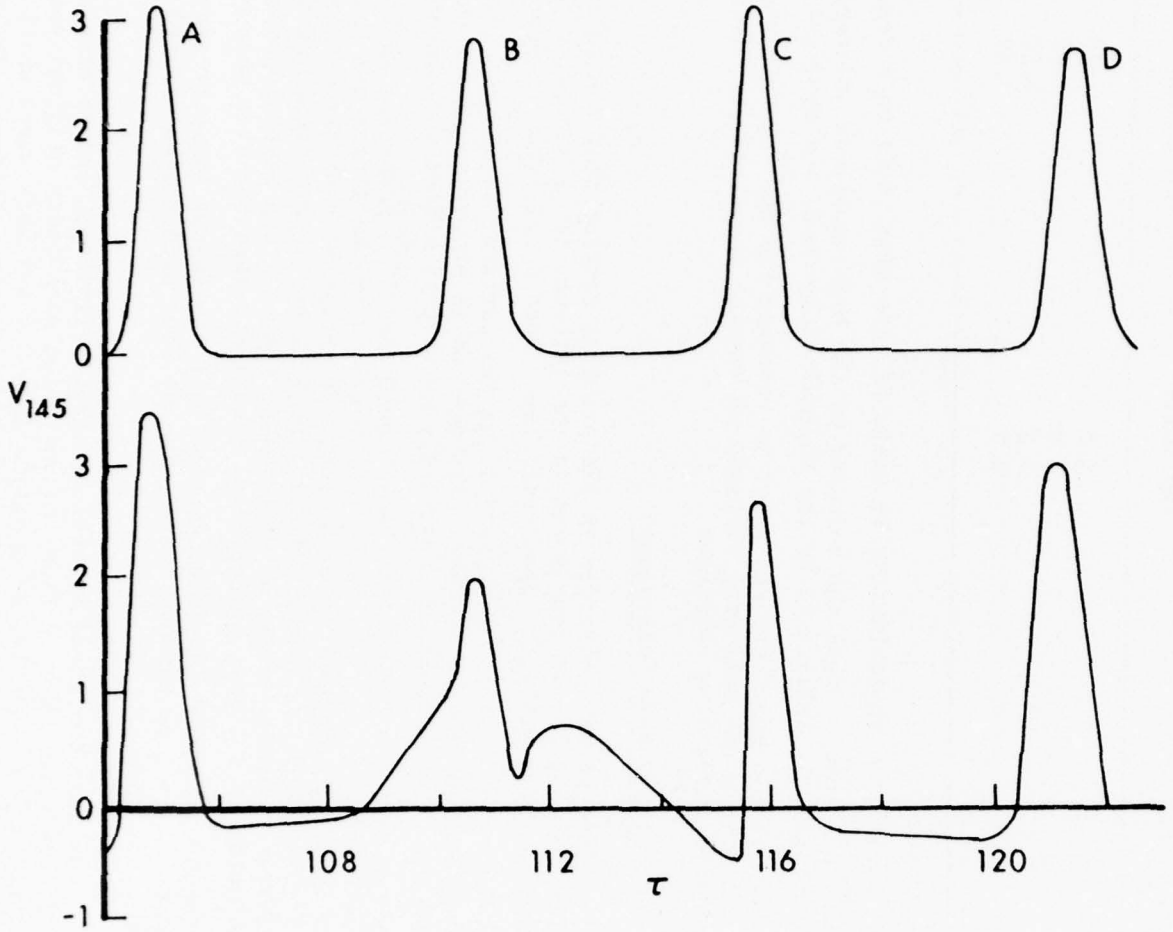

Figure 14. Propagation of solitary waves into the cold lattice. The origin of the time scale is the time at which the shock front first reaches the particle.

TABLE III. PROPAGATION VELOCITY AND AMPLITUDE OF SOLITARY WAVES. PROPAGATION VELOCITIES ARE IN PARTICLES PER UNIT OF NONDIMENSIONAL TIME.

Soliton	Amplitude	Propagation Velocity
A	3.2	1.50
B	2.9	1.42
C	3.2	1.50
D	2.7	1.38

in the lattice approximately 96 units of time after soliton B reaches the 145^{th} particle. Since the velocity of the high-amplitude solitary waves is not greatly influenced by the thermal background, our original speculation that B and C crossed prior to reaching the 300^{th} particle appears correct. In the following section, we examine the stability of the solitary waves upon collision.

6.4 Solitary-Wave Collisions

Since we have observed in the previous section that the solitary waves may collide at some point in the lattice, it is necessary to examine their stability upon collision. Such a collision is represented in Fig. 15. At the 170^{th} particle in the lattice, we see two solitary waves well separated in time. Propagation is occurring toward the left and the higher-amplitude, faster-moving wave is behind the slower one. By the time the propagation has reached the 185^{th} particle, we find that the faster-moving solitary wave has overtaken the slower one and a nonlinear interaction is occurring. It should be emphasized that the interaction is nonlinear and not just a linear superposition of the separate waves as might be expected if the solitary waves represented the solution to a linear differential equation. When the wave pair has reached the 200^{th} particle, we find that the faster solitary wave has moved completely through the slower one, but each has maintained its original shape.

We have monitored several of these collisions, and in each case the solitary waves emerged from the collision with their original shapes intact. Consequently, we conclude that the solitary waves which we observe propagating in the lattice are, in fact, solitons. The presence of these stable entities impedes the thermalization of energy behind the shock front and raises the question as to whether thermal equilibrium

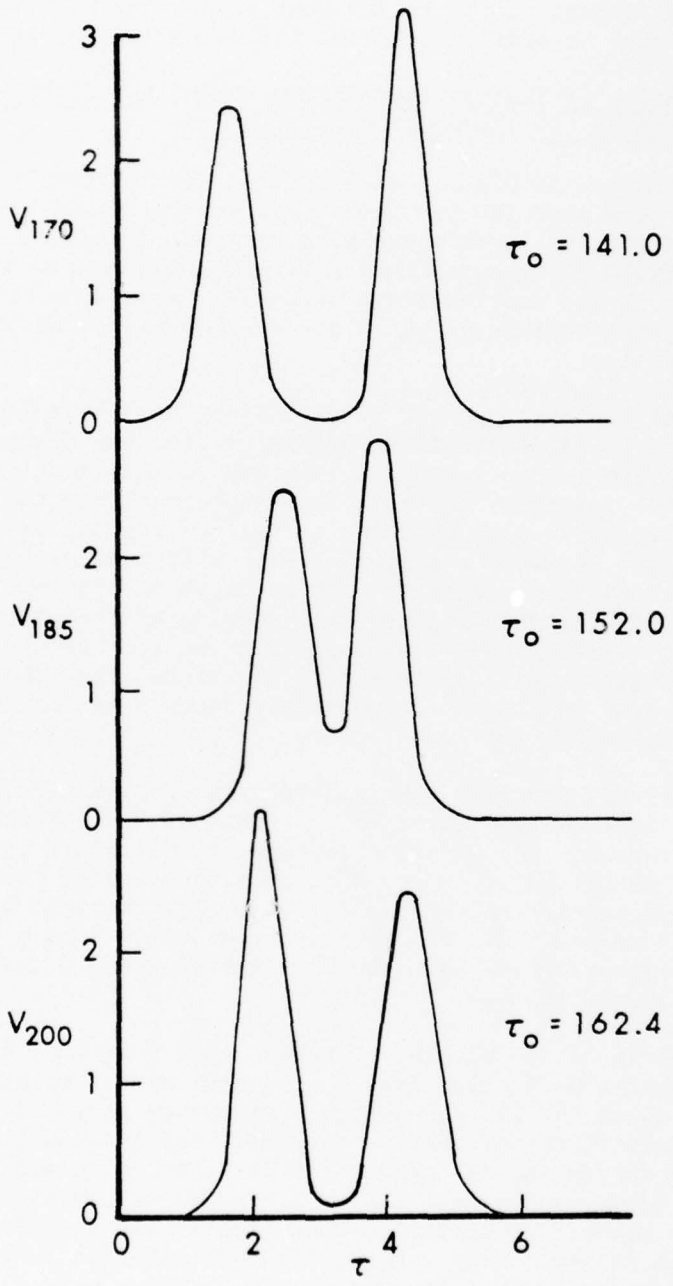

Figure 15. Velocity-time trajectories for three particles illustrating a solitary-wave collision. The origin in each case corresponds to the time represented by τ_o.

at an elevated temperature is established in the compressed lattice. This question will be addressed in the following subsection.

6.5 Investigation of Thermal Equilibrium Behind the Front and Calculation of the Thermodynamic Variables

We have plotted in Fig. 16 the profiles of the potential and kinetic energies, averaged over 100 particles, for several times. The single-particle potential and kinetic energies were calculated from the formulas indicated in Table I. The profiles exhibit a structure characteristic of shock profiles in the continuum approximation, namely, a transition region joining two regions in which the average values of the variables are roughly constant.

Because of the large number of particles which have been included in the average, it is difficult to determine from the figure whether or not the transition region increases in width as the shock propagates farther into the lattice. However, it is apparent from the discussion of the preceding subsection that the transition region, which consists of high-amplitude solitons propagating with different velocities on the thermal background, must increase with propagation distance. The growth of the transition region, owing to the spreading of the solitons, should become evident even in the averaged profiles if the calculations are extended to longer times. We conclude, therefore, that the shock profile is not steady in time as is generally assumed in continuum treatments of shock propagation in solids.

The relatively constant energy densities located well behind the front lead us to inquire whether this segment of the lattice is in thermal equilibrium. The question is somewhat difficult to answer conclusively, particularly in one dimension, because of the fairly small number of particles behind the front. If, for instance, we calculated the velocity distribution function, significant deviations from a Maxwellian function might be anticipated even if the region were in fact in equilibrium.

Nevertheless, in an attempt to answer this question, we located from Fig. 16, at a particular time τ, the approximate point behind the front at which the average energies discussed above become constant. The velocity distribution function for particles located between this point and the driven end of the lattice was then calculated. The calculation was subsequently repeated at different values of the time and for different numbers of particles contained within the sample. We consistently obtained a nearly Maxwellian distribution function which appeared to correspond to a thermal energy that was approximately a factor of 2.5 higher than the ambient thermal energy. A typical distribution function obtained is shown in Fig. 17 in which the number of atoms having velocity in a given interval is plotted. The distribution is that obtained at time τ=250, and the sample consisted of the first

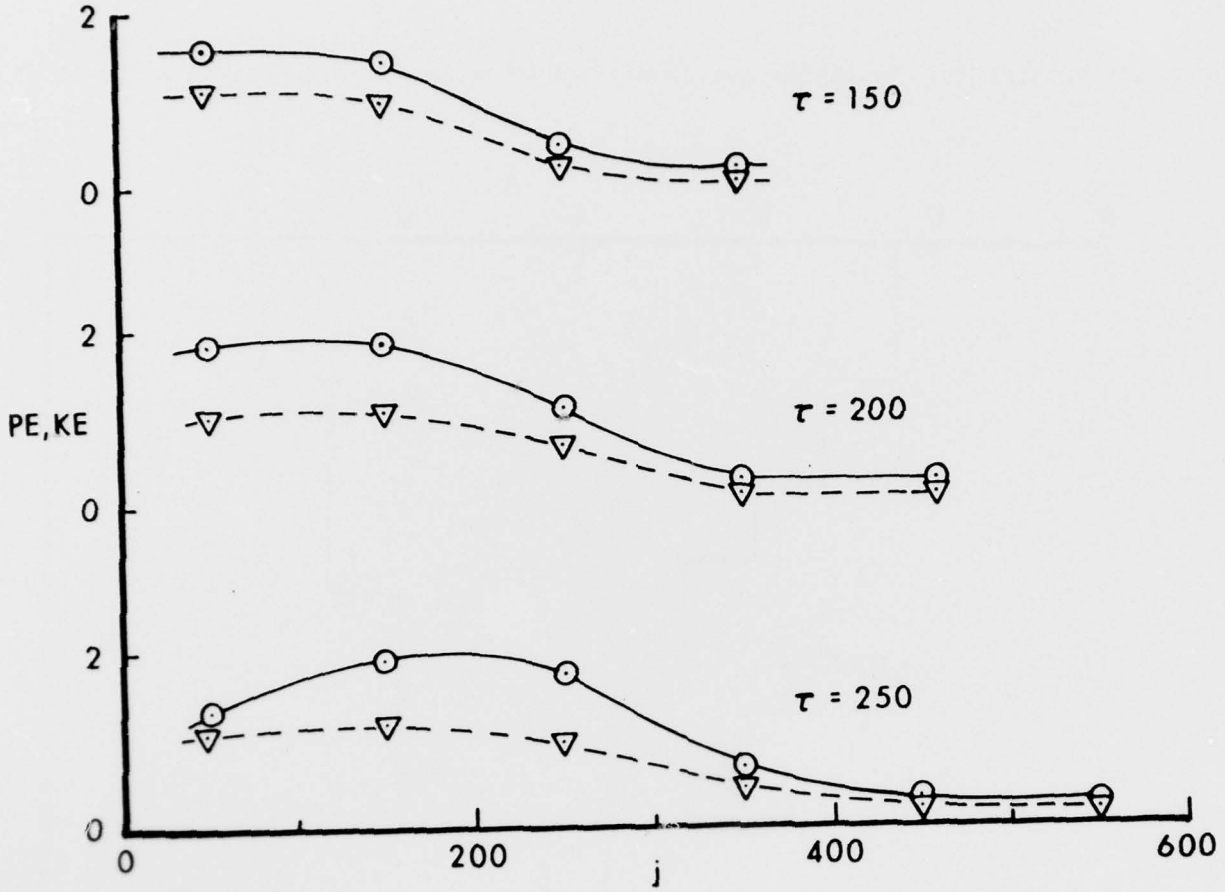

Figure 16. Average potential- and kinetic-energy profiles for the lattice with nonzero initial temperature at three times. The solid and dashed lines represent the kinetic and potential energies, respectively. The average values are plotted at the midpoint of the appropriate range.

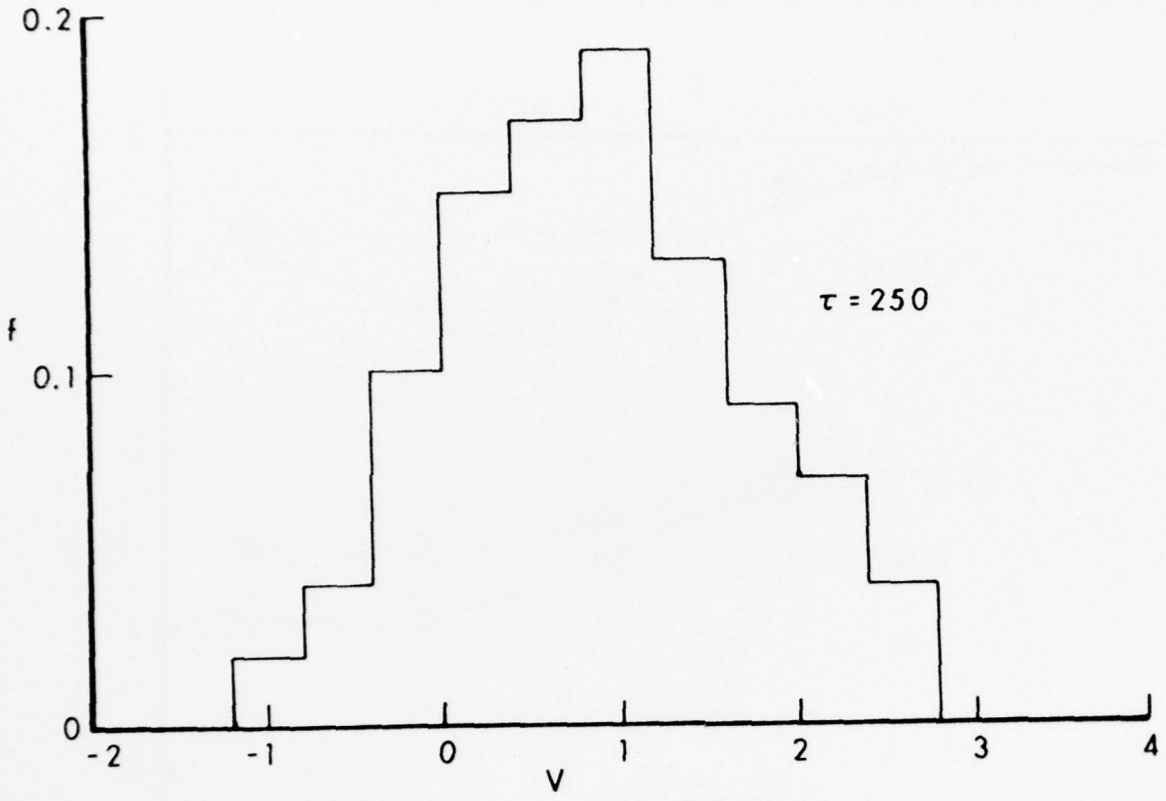

Figure 17. Velocity distribution function in the compressed region for the lattice with nonzero initial temperature.

250 particles of the lattice. The shock front at this time was around the 360^{th} particle. As can be seen from Fig. 16, the energy density is nearly constant at this time for this sample of particles. At least qualitatively, the Maxwellian character of the distribution function is obvious.

That the distribution function remains constant in time and corresponds to a higher-than-ambient temperature (See Tables IV and V.) leads us to conclude, tentatively, that some equilibration of energy occurs behind the front. For a number of reasons, however, the question has not been settled conclusively. First, it is possible that the times at which the distribution function was calculated were not sufficiently well separated to discern time-dependent behavior in the function. It is, therefore, possible that at a much longer time the function will have changed significantly. Second, it is not entirely clear whether the deviations from a theoretical Maxwellian distribution function, obvious in Fig. 17, result from the small number of particles in the sample or from an actual state of nonequilibrium. It is clear, however, that the distribution function is much more nearly Maxwellian than those obtained in Sec. 5 (zero ambient temperature), and it seems unlikely that the initial thermal oscillations could have caused so substantial a change in the function without any additional equilibration.

The question of the approach to thermal equilibrium clearly needs further investigation. We will, however, defer such investigation until the extension of the calculations to three dimensions has been made. The larger number of particles behind the front, in that case, should at least lead to a more accurate determination of the distribution function.

Assuming equilibration far behind the front, we have also calculated other thermodynamic variables both in the compressed and uncompressed, equilibrated regions of the crystal. As we have pointed out previously, the solution of the equations of motion of the particles in the lattice is independent of the equilibrium lattice spacing a_0. However, in order to calculate both the shock speed and the density within any region of the crystal, a value of this parameter must be specified. We chose a normalized value, given by

$$R = \frac{a_0 \omega_0}{u} ,$$

of 6.0 and found that the shock speed, normalized to the compression velocity, was essentially constant in time and approximately equal to 8.69. This shock speed corresponds to a Mach number of approximately 3. The pressure within a given region of the crystal was defined to be the force exerted

on the j^{th} particle by the $j+1^{st}$, averaged over the number of particles in the region under consideration. The thermal energy was defined by the expression

$$E_T = \langle (V_j - V)^2 \rangle \tag{6.14}$$

where V is the average particle velocity in the region and, here, the notation $\langle\ \rangle$ means an average over the appropriate number of particles.

The values of these thermodynamic variables, as well as the average kinetic and potential energies discussed previously, are indicated in Tables IV and V. Table IV contains the initial values or values in the uncompressed region of the lattice. In each case, these values were calculated by averaging over the last 100 particles in the lattice, all of which were located ahead of the shock. In the table, ρ is the normalized density in this region of the crystal, or the average number of particles per nondimensional lattice spacing, P is the average pressure defined previously, V is the average particle velocity, and τ is the time at which the calculation was made.

TABLE IV. VALUES OF THERMODYNAMIC VARIABLES IN UNCOMPRESSED LATTICE AT DIFFERENT TIMES. ALL VALUES WERE OBTAINED BY AVERAGING OVER THE LAST 100 PARTICLES IN THE LATTICE.

τ	V	KE	PE	E_T	ρ	P
200	0	0.32	0.18	0.32	0.167	0.96
250	0	0.28	0.22	0.28	0.165	1.22

TABLE V. VALUES OF THERMODYNAMIC VARIABLES IN COMPRESSED LATTICE AT DIFFERENT TIMES AND FOR DIFFERENT NUMBERS OF PARTICLES IN THE SAMPLE.

τ	N_s	V	KE	PE	E_T	ρ	P
200	150	0.99	1.78	1.01	0.80	0.197	5.67
	200	1.00	1.82	1.03	0.82	0.195	5.72
250	150	0.97	1.65	1.07	0.71	0.197	6.02
	200	0.93	1.56	1.11	0.70	0.197	6.19
	250	0.92	1.59	1.06	0.75	0.194	5.86

Results are obtained for three different sample sizes by averaging over the first 150, first 200, and first 250 particles in the lattice. The number of particles in the sample is indicated in the second column of the table by the parameter, N_s.

Referring first to Table IV, we see that the initial values of the various parameters are in rough agreement for the two times considered. It is likely that more exact agreement could be obtained by choosing an initial sample which contained more than 100 particles (i.e., n larger than 100 in Sec. 6.1), but it is also possible that we have not achieved complete thermal equilibrium in this segment. If not, the deviations from equilibrium were felt to be sufficiently small for practical considerations.

It is of particular interest to note in Table V that the thermal energy, E_T, behind the front is nearly constant for all samples and at both times considered. It is roughly a factor of 2.5 higher than the ambient thermal energy as we have pointed out previously. Since the thermal energy is directly proportional to the temperature, the temperature is, therefore, also a factor of 2.5 higher. We observe an increase in the density of about 20% and an increase in pressure by about a factor of 6. The average particle velocity in each of the samples is, of course, nearly equal to the compression velocity.

6.6 The Conservation Equations

If the shock profile were steady in time, the thermodynamic variables in front of and behind the shock obtained in the last subsection would satisfy the following conservation equations:

$$\rho_i \, (V_i - U_S) = \rho_f \, (V_f - U_S) \tag{6.15a}$$

$$P_i + 4\rho_i \, (V_i - U_S)^2 = P_f + 4\rho_f \, (V_f - U_S)^2 \tag{6.15b}$$

$$2E^S_i \, (V_i - U_S) \, \rho_i + P_i \, (V_i - U_S) = 2E^S_f \, (V_f - U_S) \, \rho_f + P_f (V_f - U_S) \, . \tag{6.15c}$$

In these equations, U_S denotes the shock speed, which is approximately 8.69 as discussed earlier, and i and f denote initial values in front of the shock (Table IV) and final values behind the shock (Table V), respectively. The quantity E^S is the total energy measured in the shock frame and is related to the potential and kinetic energies in the lab frame through the formula

$$E^S = PE + KE - 2VU_S + U_S^2 \quad . \tag{6.16}$$

Equations (6.15) can be derived from more general hydrodynamic equations[47]; when considered in conjunction with an equation of state, they yield the so-called Hugoniot conditions[48].

Although, as we have stressed earlier, the profile is not steady in time, it is of interest to determine the extent to which Eqs. (6.15) are satisfied. To do so, we checked the conservation equations at τ=250 using the data from Tables IV and V. The final values were taken to be the averages over the first 250 particles in the lattice (last row, Table V). The equations were then checked by directly substituting for the variables in Eqs. (6.15) and comparing the right- and left-hand sides of the equations.

The results are indicated in Table VI. Column 1 lists the equation number, column 2 the value obtained for the left-hand side of the equation, column 3 the corresponding value for the right-hand side, and column 4 the percent deviation. The last figure was calculated by taking the absolute value of the ratio of the difference in the right- and left-hand sides to the value of the left-hand side. It is rather interesting that the largest deviations are around 5%, suggesting that the nonsteady behavior of the profile affects the Hugoniot conditions only slightly. A similar conclusion has been reached by Tsai.

TABLE VI. STEADY-STATE CONSERVATION EQUATIONS

Equation #	LHS	RHS	% Deviation
6.15a	-1.43	-1.50	5%
6.15b	51.03	52.58	3%
6.15c	-228.49	-232.47	2%

47. D.A. Desloge, Statistical Physics (Holt, Reinhart, and Winston, New York, 1966), Chap. 12.
48. H.W. Liepmann and A. Roshko, Elements of Gasdynamics (Wiley, New York, 1957), Chap. 4.

7. SUMMARY, CONCLUSIONS, AND FUTURE INVESTIGATIONS

We have carried out numerical and some analytic calculations describing shock propagation in a one-dimensional, discrete lattice. A number of interatomic potentials have been studied, but the most extensive treatment has been given to the case in which the atoms interact via a Morse-type potential. Two special cases of initial conditions have been considered. In the first, we assumed the atoms were initially at rest in their equilibrium positions (zero ambient temperature) prior to being excited by the shock; in the second, the lattice was initially in thermal equilibrium with an energy that corresponded roughly to room temperature.

The major conclusions which can be drawn from the calculations are as follows:

1. In no cases studied was the shock profile found to be steady in time as is generally assumed in continuum calculations. The cause of the nonsteady behavior is the propagation of well-defined pulses (solitary waves) behind the front whose propagation velocity varies with amplitude. The difference in propagation velocity of different solitons introduces a spreading effect which apparently prevents the profile from ever approaching a steady state.

2. For the initially quiescent lattice, no equilibration of energy occurs behind the shock front and there is, consequently, no temperature rise. All energy introduced by the shock wave is either potential or ordered translational energy.

3. For a lattice with a nonzero initial temperature, thermalization of energy behind the front does appear to occur but this aspect of the problem requires further investigation. The profile, however, is still nonsteady and the transition region between the two equilibrated parts of the lattice grows with time. Again, the growth results from the spreading effect of solitary waves of different amplitudes and propagation velocities.

In the future, we intend to extend the calculations to a three-dimensional model to see if similar effects will persist in that case. Recently, Zabusky[49] has interpreted an increase in thermal conduction with the addition of anharmonicities, observed by Payton, Rich, and Visscher[50], as resulting from the propagation of solitons in the model studied. That model was two dimensional (as well as isotopically impure) and it therefore appears reasonable to expect that soliton propagation might be an important effect in a three-dimensional model as well.

---

49. N.J. Zabusky, "Solitons and Energy Transport in Nonlinear Lattices", Computer Phys. Comm. 5, 1 (1973).
50. D.N. Payton III, M. Rich, and W.M. Visscher, "Lattice Thermal Conductivity in Disordered Harmonic and Anharmonic Crystal Models", Phys. Rev. 160, 706 (1967).

If so, we believe that the effects may be significant in the study of shock-induced detonations. In most current theories, the effect of the shock front is ignored entirely and the only function the shock has is to raise the temperature, pressure, and density of the solid to higher-than-ambient values. Chemical reactions are then assumed to occur in the thermally equilibrated part of the crystal behind the front. It would appear, however, that if the transition region grows in time, reactions may occur in a region of the crystal characterized by an extreme state of nonequilibrium, and it is important to assess the effects of this nonequilibrium environment upon chemical-reaction rates. It is unlikely, for instance, that such rates can be represented by an Arrhenius-type relation whose validity is dependent upon the assumption of equilibrium. Furthermore, the solitons at the shock front lead to particle velocities significantly higher than the velocities typically found in the equilibrated regions of the compressed crystal, an effect which may be significant in understanding the initiation process in explosives.

It would also be desirable in the future to study the properties of solitons in more detail than has been possible in this report. Of particular interest would be to study the effects of random thermal oscillations upon the propagation of solitons of different amplitude. Such a study would perhaps lend insight into why (or why not) equilibration of energy occurs behind the front in the case of the initially equilibrated lattice. It would also be interesting to study the effects of perturbations transverse to the propagation direction of the soliton (in a two- or three-dimensional model). It would appear that only the absence of stability under such perturbations could prevent soliton propagation from being an important effect in more realistic, three-dimensional crystals.

ACKNOWLEDGMENTS

We wish to express our appreciation to Professors M.D. Kruskal and N.J. Zabusky for their helpful comments regarding the interpretation of this work and for their hospitality during our visit to Princeton. We are also grateful to Dr. D.H. Tsai for instructing us in the method of calculation discussed in Sec. 6.1, and to our colleague, Dr. D.F. Strenzwilk, for several useful discussions. The computational assistance afforded us by Drs. G.F. Adams, P. Deutsch, and D.A. Ringers is gratefully acknowledged. Finally, we wish to thank Dr. D. Eccleshall, BRL, for his interest in this work and for his constant support and encouragement.

REFERENCES

1. R. Becker, "Stosswelle und Detonation", Z. Physik 8, 321 (1922).

2. H.M. Mott-Smith, "The Solution of the Boltzmann Equation for a Shock Wave", Phys. Rev. 82, 885 (1951).

3. G.A. Bird, "Aspects of the Structure of Strong Shock Waves", Phys. Fluids 13, 1172 (1970).

4. D.H. Tsai, "An Atomistic Theory of Shock Compression of a Perfect Crystalline Solid", in Accurate Characterization of the High-Pressure Environment, edited by E.C. Lloyd, Natl. Bur. Stds. Spec. Publ. No. 326 (U.S. GPO, Washington, DC, 1971), p. 105.

5. W. Band, "Studies in the Theory of Shock Propagation in Solids", J. Geophys. Res. 65, 695 (1960).

6. D.R. Bland, "On Shock Structure in a Solid", J. Inst. Math. Applications 1, 56 (1965).

7. E. Fermi, J.R. Pasta, and S.M. Ulam, "Studies in Nonlinear Problems", Los Alamos Sci. Lab. Rep. LA-1940, 1955; also in Collected Works of Enrico Fermi (Univ. Chicago Press, Chicago, 1965), V. II, p. 978.

8. B. Lewis and G. von Elbe, Combustion, Flames, and Explosion of Gases (Academic, New York, 1951), Chap. XI.

9. D.H. Tsai and C.W. Beckett, "Shock Wave Propagation in Cubic Lattices", J. Geophys. Res. 71, 2601 (1966).

10. D.H. Tsai and R.A. MacDonald, "Second Sound in a Solid Under Shock Compression", J. Phys. C 6, L171 (1973).

11. J.C. Ward and J. Wilks, "Second Sound and the Thermo-Mechanical Effect at Very Low Temperatures", Phil. Mag. 43, 48 (1952).

12. M. Chester, "Second Sound in Solids", Phys. Rev. 131, 2013 (1963).

13. J.M. Ziman, Electrons and Phonons (Oxford University Press, London 1960), Chap. III.

14. A. Paskin and G.J. Dienes, "Molecular Dynamic Simulations of Shock Waves in a Three-Dimensional Solid", J. Appl. Phys. 43, 1605 (1972).

15. A. Paskin and G.J. Dienes, "A Model for Shock Waves in Solids and Evidence for a Thermal Catastrophe", Solid State Comm. 17, 197 (1975).

16. R. Manvi, G.E. Duvall, and S.C. Lowell, "Finite Amplitude Longitudinal Waves in Lattices", *Int. J. Mech. Sci.* 11, 1 (1969).

17. G.E. Duvall, R. Manvi, and S.C. Lowell, "Steady Shock Profile in a One-Dimensional Lattice", J. Appl. Phys. 40, 3771 (1969).

18. R. Manvi and G.E. Duvall, "Shock Waves in a One-Dimensional, Non-Dissipating Lattice", Brit. J. Appl. Phys. 2, 1389 (1969).

19. J. Tasi, "Perturbation Solution for Growth of Nonlinear Shock Waves in a Lattice", J. Appl. Phys. 43, 4016 (1972). See also Erratum [J. Appl. Phys. 44, 1414 (1973)].

20. J. Tasi, "Far-Field Analysis of Nonlinear Shock Waves in a Lattice", J. Appl. Phys. 44, 4569 (1973).

21. J. Tasi, "Perturbation Solution for Shock Waves in a Dissipative Lattice", J. Appl. Phys. 44, 2245 (1973).

22. P. Choquard, The Anharmonic Crystal (Benjamin, New York, 1967), Chap. 6.

23. R.S. Northcote and R.B. Potts, "Energy Sharing and Equilibrium for Nonlinear Systems", J. Math. Phys. 5, 383 (1964).

24. P.M. Morse and K.U. Ingard, Theoretical Acoustics (McGraw-Hill, New York, 1968), Chap. 3.

25. R. Weinstock, "Propagation of a Longitudinal Disturbance on a One-Dimensional Lattice", Am. J. Phys. 38, 1289 (1970).

26. E.M. Baroody and E. Drauglis, "Propagation of a Sharp Disturbance Along a One-Dimensional Lattice", Am. J. Phys. 39, 1412 (1971).

27. A.H. Nayfeh and M.H. Rice, "On The Propagation of Disturbances in a Semi-Infinite One-Dimensional Lattice", Am. J. Phys. 40, 469 (1972).

28. F.O. Goodman, "Propagation of a Disturbance on a One-Dimensional Lattice Solved by Response Functions", Am. J. Phys. 40, 92 (1972).

29. E. Schroedinger, "Zur Dynamik Elastisch Gekoppelter Punktsysteme", Ann. Phys. 44, 916 (1914).

30. Handbook of Mathematical Functions, edited by M. Abramowitz and I. Stegun (Natl. Bur. Std., Washington, DC, 1964), Chap. 9.

31. B. Carnahan, H.A. Luther, and J.O. Wilkes, Applied Numerical Methods (Wiley, New York, 1969), Chap. 6.

32. A. Ralston, A First Course in Numerical Analysis (McGraw-Hill, New York, 1965), Chap. 5.

33. R. Manvi, "Shock Wave Propagation in a Dissipating Lattice Model", Ph.D. Thesis (Washington State University, 1968) (Unpublished).

34. N.J. Zabusky and M.D. Kruskal, "Interaction of Solitons in a Collisionless Plasma and the Recurrence of Initial States", Phys. Rev. Letters 15, 240 (1965).

35. D.F. Strenzwilk, "Effect of Different Initial Accelerations on the Subsequent Shock Profile in One-Dimensional Lattices", BRL Report (to be published).

36. M. Toda, "Vibration of a Chain With Nonlinear Interaction", J. Phys. Soc. Japan 22, 431 (1967).

37. M. Toda, "Wave Propagation in Anharmonic Lattices", J. Phys. Soc. Japan 23, 501 (1967).

38. A.C. Scott, F.Y.F. Chu and D.W. McLaughlin, "The Soliton: A New Concept in Applied Science", Proc. IEEE 61, 1443 (1973).

39. M. Toda, "Studies in a Nonlinear Lattice", Physics Reports 18C, 1 (1975).

40. R.C. Tolman, The Principles of Statistical Mechanics (Oxford University Press, New York, 1938), Chap. 3.

41. J. Ford, "Equipartition of Energy for Nonlinear Systems", J. Math. Phys. 2, 387 (1961).

42. J. Ford and J. Waters, "Computer Studies of Energy Sharing and Ergodicity for Nonlinear Oscillator Systems", J. Math. Phys. 4, 1293 (1963).

43. E.A. Jackson, "Nonlinear Coupled Oscillators. I. Perturbation Theory; Ergodic Problem", J. Math. Phys. 4, 551 (1963).

44. E. Montroll, in "Proceedings of the Explosives Chemical Reactions Seminar", ARO-D Report 70-4, Durham, NC, 1968, p. 145.

45. D.H. Tsai, private communication.

46. B.J. Alder and T.E. Wainwright, "Studies in Molecular Dynamics. I. General Method", J. Chem. Phys. 31, 459 (1959).

47. D.A. Desloge, Statistical Physics (Holt, Reinhart, and Winston, New York, 1966), Chap. 12.

48. H.W. Liepmann and A. Roshko, Elements of Gasdynamics (Wiley, New York, 1957), Chap. 4.

49. N.J. Zabusky, "Solitons and Energy Transport in Nonlinear Lattices", Computer Phys. Comm. 5, 1 (1973).

50. D.N. Payton III, M. Rich, and W.M. Visscher, "Lattice Thermal Conductivity in Disordered Harmonic and Anharmonic Crystal Models", Phys. Rev. 160, 706 (1967).

DISTRIBUTION LIST

No. of Copies	Organization
12	Commander Defense Documentation Center ATTN: DDC-TCA Cameron Station Alexandria, VA 22314
1	Commander US Army Materiel Development and Readiness Command ATTN: DRCDMA-ST 5001 Eisenhower Avenue Alexandria, VA 22333
1	Commander US Army Aviation Research and Development Command ATTN: DRSAV-E 12th and Spruce Streets St. Louis, MO 63166
1	Director US Army Air Mobility Research and Development Laboratory Ames Research Center Moffett Field, CA 94035
1	Commander US Army Electronics Command ATTN: DRSEL-RD Fort Monmouth, NJ 07703
1	Commander US Army Missile Research and Development Command ATTN: DRDMI-R Redstone Arsenal, AL 35809
1	Commander US Army Tank Automotive Development Command ATTN: DRDTA-RWL Warren, MI 48090
1	Commander US Army Mobility Equipment Research & Development Cmd ATTN: Tech Docu Cen, Bldg 315 DRSME-RZT Fort Belvoir, VA 22060
1	Commander US Army Armament Materiel Readiness Command Rock Island, IL 61202
1	Commander US Army Armament Research and Development Command ATTN: Dr. P. Harris Dover, NJ 07801
1	Commander US Army Harry Diamond Labs ATTN: DRXDO-TI 2800 Powder Mill Road Adelphi, MD 20783
1	Director US Army Materials and Mechanics Research Center ATTN: Dr. R. Harrison Watertown, MA 02172
1	Director US Army TRADOC Systems Analysis Activity ATTN: ATAA-SA White Sands Missile Range NM 88002
1	Commander Army Research and Standardization Group (Europe) Electronics Branch ATTN: Dr. Alfred K. Nedoluha Box 65 FPO New York 09510

DISTRIBUTION LIST

No. of Copies	Organization
2	Director Lawrence Livermore Laboratory ATTN: Dr. W. Hoover Dr. A. Karo Livermore, CA 94550
3	Director National Bureau of Standards ATTN: Dr. H. Prask Dr. S. Trevino Dr. D. Tsai Gaithersburg, MD 20760
1	Science Applications, Inc. ATTN: Mr. S. Howie 2028 Powers Ferry Rd, Suite 260 Atlanta, GA 30339
1	Massachusetts Institute of Technology Dept. of Nuclear Engineering ATTN: Professor S. Yip Cambridge, MA 02139
1	Princeton University Astrophysics Department Professor M.D. Kruskal Princeton, NJ 08540
1	Queens College ATTN: Professor A. Paskin Flushing, NY 11973
1	State University of New York Department of Mechanics ATTN: Professor J. Tasi Stony Brook, NY 11790
1	University of California at Irvine Department of Physics ATTN: Dr. A. Maradudin Irvine, CA 92664
3	University of Florida Department of Engineering Sciences ATTN: Prof. K.T. Millsaps Prof. D.R. Keefer Prof. B.M. Leadon Gainesville, FL 32603
1	University of Massachusetts Department of Physics ATTN: Professor R. Guyer Amherst, MA 01002
1	University of Pittsburgh ATTN: Prof. N.J. Zabusky Pittsburgh, PA 15260
1	University of Rochester Department of Physics & Astronomy ATTN: Professor E. Montroll Rochester, NY 14627
1	University of Wisconsin Department of Electrical and Computer Engineering ATTN: Prof. A. Scott Madison, WI 53706
1	Washington State University Shock Dynamics Laboratory ATTN: Prof. G. Duvall Pullman, WA 99163
	Aberdeen Proving Ground
	Marine Corps Ln Ofc Dir, USAMSAA